

As a library, NLM provides access to scientific literature. Inclusion in an NLM database does not imply endorsement of, or agreement with, the contents by NLM or the National Institutes of Health.

Learn more: [PMC Disclaimer](#) | [PMC Copyright Notice](#)



[Astrobiology](#). 2015 Jan 1;15(1):32–56. doi: [10.1089/ast.2014.1210](https://doi.org/10.1089/ast.2014.1210)

## Spaceflight Induces Specific Alterations in the Proteomes of *Arabidopsis*

[Robert J Ferl](#)<sup>1,,2,✉</sup>, [Jin Koh](#)<sup>2</sup>, [Fiona Denison](#)<sup>1</sup>, [Anna-Lisa Paul](#)<sup>1</sup>

[Author information](#) [Article notes](#) [Copyright and License information](#)

PMCID: PMC4290804 PMID: [25517942](https://pubmed.ncbi.nlm.nih.gov/25517942/)

### Abstract

---

Life in spaceflight demonstrates remarkable acclimation processes within the specialized habitats of vehicles subjected to the myriad of unique environmental issues associated with orbital trajectories. To examine the response processes that occur in plants in space, leaves and roots from *Arabidopsis thaliana* seedlings from three GFP reporter lines that were grown from seed for 12 days on the International Space Station and preserved on orbit in RNAlater were returned to Earth and analyzed by using iTRAQ broad-scale proteomics procedures. Using stringent criteria, we identified over 1500 proteins, which included 1167 leaf proteins and 1150 root proteins we were able to accurately quantify. Quantification revealed 256 leaf proteins and 358 root proteins that showed statistically significant differential abundance in the spaceflight samples compared to ground controls, with few proteins differentially regulated in common between leaves and roots. This indicates that there are measurable proteomics responses to spaceflight and that the responses are organ-specific. These proteomics data were compared with transcriptome data from similar spaceflight samples, showing that there is a positive but limited relationship between transcriptome and proteome regulation of the overall spaceflight responses of plants. These results are discussed in terms of emergence understanding of plant responses to spaceflight particularly with regard to cell wall remodeling, as well as in the context of deriving multiple omics data sets from a single on-orbit preservation and operations approach. Key Words: Space biology—Proteomics—

## 1. Introduction

---

PLANTS UNDERGO substantial physiological adaptation to accommodate changing environments. As sessile organisms, plants have developed exquisitely sensitive metabolisms that can provide insights into how eukaryotes sense and respond to external stimuli. Spaceflight presents unique challenges to terrestrial organisms. The microgravity environment in itself is outside the evolutionary experience of any terrestrial organism, but the absence of gravity also impacts the physical environment inherent to the unique living space of orbital vehicles (Musgrave *et al.*, 1997; Wolff *et al.*, 2013). It is now well established that plants grown in orbital vehicles exhibit significant changes in gene expression as part of the physiological adaptation to the spaceflight environment (Link *et al.*, 2001; Paul *et al.*, 2001, 2005, 2012b, 2013; Stutte *et al.*, 2006; Salmi and Roux, 2008; Salmi *et al.*, 2011; Correll *et al.*, 2013; Nasir *et al.*, 2014; Sugimoto *et al.*, 2014).

However, studies approaching plant adaptation to spaceflight at the level of the proteome have been limited. To date, the only true proteomic-scale study of plants in space has been a label-free analysis of membrane proteins isolated from Arabidopsis seedlings grown on the International Space Station (ISS) (Mazars *et al.*, 2014). The distribution of differentially abundant proteins among three treatments (microgravity of the ISS, a 1g orbital centrifuge, and a 1g ground control) highlights familiar pathways in gravity signal transduction. Many of the membrane-associated proteins involved in auxin signaling cascades were less prominent in microgravity-grown plants, while many proteins typically associated with stress responses were more abundant. While there is not a one-to-one correlation with any gene set from a published spaceflight transcriptome, similar trends in the differential expression of genes important to auxin metabolism, and to a variety of stress responses, can be seen in the transcription profiles from several studies (see citations above). A proteomic survey in terrestrial altered-gravity environments also revealed a host of general stress proteins as well as those associated with auxin signaling (Tan *et al.*, 2011). Although there is little specific overlap with transcriptome studies of plants exposed to similar environments, many of the trends in pathways affected by spaceflight are similar among the studies (Moseyko *et al.*, 2002; Tan *et al.*, 2011). With increased technical sensitivity and better access to space, the spaceflight responses contribute to a comprehensive picture of the strategies used by plants to cope with changes in their environment.

Comparative proteomics mass spectrometry (MS) methods can be used to reveal quantitative changes in the protein complement of cells and organs over a large scale between and among samples. The use of iTRAQ (isotope tags for relative and absolute quantification; Applied Biosystems) allows for quantitative comparisons of samples by labeling lysine residues and N-termini of peptides with mass reporter molecules, such that the samples can be combined into simultaneous analyses by MS. The relative amounts of every identified peptide from each sample are simultaneously revealed within the tandem mass spectra through the relative intensity of the differentially labeled ion peaks, enabling each peptide to be correlated to each sample through the mass of the reporter molecules. Several papers have

demonstrated the effectiveness of iTRAQ analysis of Arabidopsis samples in the study of broad-scale proteomic changes (Zhao *et al.*, 2010; Alvarez *et al.*, 2011; Schenck *et al.*, 2013; Li *et al.*, 2014).

The major scientific goal of this study was to discover proteomics changes that characterize the physiological adaptation of Arabidopsis to the spaceflight environment. To accomplish this goal, we sought to examine proteomics changes on an organ-specific level by comparing the proteomics of roots and leaves between plants grown in space and plants grown on Earth. The samples were from Arabidopsis seedlings from three green fluorescent protein (GFP) lines that were germinated on the ISS and grown for 12 days before being preserved in the strong protein denaturant RNAlater and then frozen. The nature of these samples, having been preserved in RNAlater primarily for gene expression analyses, necessitated the development of methods for protein extraction from RNAlater samples and the processing of small amounts of proteins through iTRAQ and MS analyses. Therefore, the secondary and technical goal of this study was to examine proteomics based on samples from this preservation method, which is widely used in ISS spaceflight biology research, to discern whether this form of preservation could enable broad-scale proteomics of spaceflight samples. The resulting data demonstrate the technical success of the approach and show significant spaceflight-induced proteomic changes that were different between roots and leaves. These proteomics data are discussed in the context of adaptive physiologies in space and are also discussed in relation to gene expression changes that have been seen in similar plants in space.

## 2. Materials and Methods

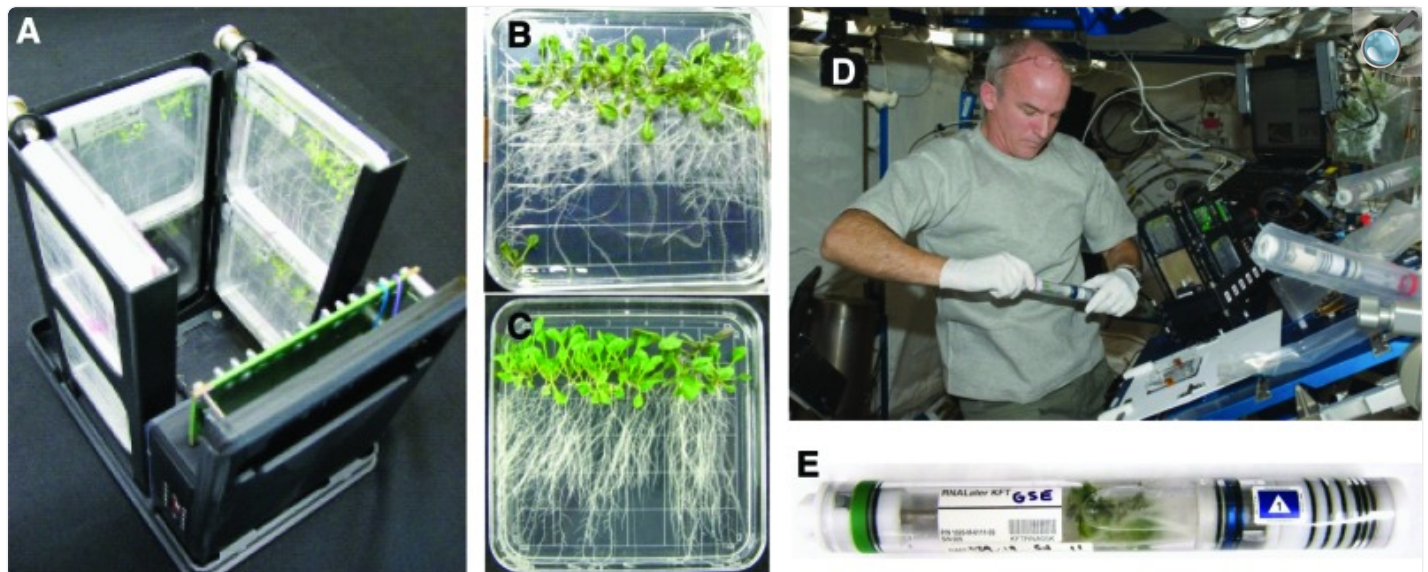
---

### 2.1. Plant growth and harvest on the ISS

The data presented here are from plants harvested during one of several experiments launched to the ISS on STS-129, November 16, 2009 (specifically, Run 1B: 12/3/2009–12/15/2009), and returned on STS-130, February 8, 2010. Arabidopsis seeds were planted aseptically on the surface of 10 cm<sup>2</sup> solid media plates (Paul *et al.*, 2004). The samples come from a collection of three Arabidopsis lines. The three GFP [green fluorescent protein (Sheen *et al.*, 1995)] reporter gene lines were Adh::GFP [alcohol dehydrogenase promoter (Manak *et al.*, 2002)]; DR5r::GFP [synthetic auxin response element composed of five AuxRE elements; gift of T. Guilfoyle (Ulmasov *et al.*, 1997)]; and 35s::GFP [driven by the CaMV35s promoter (Manak *et al.*, 2002)]. Seeds and seeded plates were prepared in such a way as to maintain dormancy in light-tight coverings until the initiation of the experiment on orbit (Paul *et al.*, 2012a). The plated seeds remained dormant until activated by exposure to light on the ISS, which initiated germination. Both the flight plates and ground control plates were grown in the Advanced Biological Research System, ABRS (NASA, 2011a; Paul *et al.*, 2012a, 2013). The ABRS provided temperature control, light control, and circulation of air that was scrubbed to remove volatile organic compounds. On orbit, the dormant seeded plates were unwrapped from their coverings and installed in the GFP Imaging System (GIS) (Fig. 1A), which was then inserted into the ABRS. The GIS held the plates within the ABRS, facilitated access by the astronaut on orbit, and provided regular imaging (NASA, 2011b; Paul *et al.*, 2012a). After growth, all plates were photographed by the crew (Fig. 1B), along with the comparable GIS/ABRS-grown ground

control (Fig. 1C). The plates were then harvested on orbit to RNAlater-filled Kennedy Space Center Fixation Tubes (KFTs) (Fig. 1D and 1E) and then stowed below  $-80^{\circ}\text{C}$  in the MELFI freezer on the ISS (Ferl *et al.*, 2011) before return. The ground control plates were similarly housed in the GIS of an ABRS in the Orbital Environmental Simulator chamber in the Spaceflight Life Sciences Laboratory at Kennedy Space Center following a similar, but delayed, timeline as the plates on the ISS, with the use of environmental data such as temperature, relative humidity, light levels, and  $\text{CO}_2$  concentrations as was experienced by the plants on orbit. Further details on the operational outlines can be found in Paul *et al.* (2012a, 2013). The ground control samples received the same physical processing steps of harvest, freezing, thawing, and distribution in the laboratory as did the spaceflight samples.

**FIG. 1.**



[Open in a new tab](#)

Plant growth, hardware, harvesting, and preservation in RNAlater on the ISS. The Petri plates within which the plants were grown were housed in the GIS unit of the ABRS (A). A representative flight (B) and ground control (C) plate are shown, along with astronaut Jeff Williams harvesting plates on the ISS (D) for preservation in RNAlater in a KFT (E) before freezing on orbit. (Color images available online at [www.liebertonline.com/ast](http://www.liebertonline.com/ast) )

## 2.2. Isolation of proteins from RNAlater-preserved *Arabidopsis*

The 12-day-old plants recovered from the frozen KFTs of both flight and ground control plants were thawed then

dissected into roots, hypocotyls, and leaves, similar to the dissections performed by Paul *et al.* (2013). Approximately half the root material from 6–7 seedlings within a single Petri plate constituted each of three biological replicates for analysis of root proteins. For each replicate, 80 mg of RNAlater-fixed Arabidopsis root material was blotted with tissue to remove excess RNAlater and then ground in a liquid nitrogen–chilled pestle and mortar with 400 µL protein extraction buffer per sample [100 mM sodium phosphate (pH 7), 2 mM EDTA, 25 mM NaF, 5 mM MgCl<sub>2</sub>, 150 mM NaCl, 0.1% triton-X100, 10% glycerol, 1 mM dithiothreitol], commercial cocktails of protease (Set VI, Calbiochem) and phosphatase (Set I, Calbiochem) inhibitors. Samples were ground until completely homogeneous and then centrifuged at 13,000 rpm for 10 min at 4°C. The supernatant containing buffer-soluble proteins was collected, and proteins were purified as described by Koh *et al.* (2012). The leaf sample from flight and ground control plants was similarly prepared from half the material of a single Petri plate, constituting the leaves from seven plants. Protein assays were performed to quantify purified proteins by using the Pierce BCA Protein Assay Kit (Thermo Scientific, Rockford, IL, USA) with the SoftMax Pro Software v5.3 (Molecular Devices, Downingtown, PA, USA) under the SpectraMax M5 (Molecular Devices).

### 2.3. Protein digestion, iTRAQ labeling, and MS

For each sample (three replicate root samples and the single leaf sample for the flight and ground controls), 16 µg of the recovered proteins were reduced, alkylated, trypsin-digested, and labeled according to the manufacturer's instructions (AB Sciex Inc.). The three biological replicates of ground root samples were labeled with iTRAQ tags 113, 114, and 115, and those of flight root samples were labeled with 116, 117, and 118, respectively. The ground shoot sample was labeled with iTRAQ tag 119, while the flight shoot was labeled with 121. The combined labeled peptide mixtures were desalted with C18-solid phase extraction and dissolved in strong cation exchange solvent A [25% (v/v) acetonitrile, 10 mM ammonium formate, and 0.1% (v/v) formic acid (pH 2.8)]. The peptides were fractionated by an Agilent HPLC system 1260 with a polysulfoethyl A column (2.1×100 mm, 5 µm, 300 Å; PolyLC, Columbia, MD, USA) with a flow rate of 200 µL/min. Peptides were eluted with a linear gradient of 0–20% solvent B [25% (v/v) acetonitrile and 500 mM ammonium formate (pH 6.8)] over 50 min followed by ramping up to 100% solvent B in 5 min. Fourteen fractions were collected by monitoring the absorbance at 280 nm and lyophilized ([Supplementary Fig. S1](#); supplementary data are available online at [www.liebertonline.com/ast](http://www.liebertonline.com/ast) ).

A quadrupole-time-of-flight LTQ Orbitrap XL MS/MS system (Thermo Fisher Scientific, Bremen, Germany) was used for data acquisition as described previously (Makarov *et al.*, 2006). It was interfaced with an Eksigent nano-LC AS2 system (Eksigent Technologies, Dublin, CA, USA) using high-energy collision dissociation. Each fraction was loaded onto an Agilent Zorbax 300SB-C18 trap column (0.3 mm i.d.×5 mm length, 5 µm particle size) with a flow rate of 5 µL/min for 10 min. Reversed-phase C<sub>18</sub> chromatographic separation of peptides was carried out on a pre-packed BetaBasic C<sub>18</sub> PicoFrit column (75 µm i.d.×10 cm length, New Objective, Woburn, MA, USA) at 300 nL/min with the following gradient: 5% B for 1 min as an equilibration status; 60% B for 99 min as a gradient; 90% B for 5 min as a washing status; 5% B for 10 min as an equilibration status (solvent A: 0.1% formic acid in 97% water, 3% acetonitrile; solvent B:

0.1% formic acid in 97% acetonitrile, 3% water).

## 2.4. Proteomics analyses

The MS/MS data were processed by a thorough search considering biological modification and amino acid substitution against the non-redundant uniprot *Arabidopsis thaliana* database (53,270 entries downloaded on June 14, 2014, at <http://beta.uniprot.org>) by using the Fraglet and Taglet searches under the Paragon algorithm (Shilov *et al.*, 2007) of ProteinPilot v.4.5 software (AB Sciex, Inc.) and Sequest search (Eng *et al.*, 1994) under Proteome Discoverer v.1.4 software (Thermo Scientific, Inc.). Mascot searches (Perkins *et al.*, 1999) under Mascot Daemon (Matrix Science, Boston, MA, USA) were conducted with the following parameters: trypsin digestion allowing for up to two missed cleavages, methionine oxidation and iTRAQ on N-termini and lysines, iTRAQ 8-plex quantification, 10 ppm tolerance for MS and MS/MS, peptide charges of +1, +2, and +3, and monoisotopic masses. Plant protein, cysteine modification with methyl methanethiosulfate, fixed iTRAQ modification of free amine in the N-terminus and lysine, and variable iTRAQ modifications of tyrosine were considered. ProteoIQ2.7 (PREMIER Biosoft, Palo Alto, CA, USA) was used to cluster peptides to proteins (protein groups) and output lists of proteins having a minimum peptide probability of >0.95 and a minimum protein probability of <0.95 from all search results for final identification at a 5% false discovery rate (FDR; for comparison of FDRs, see [Supplementary Fig. S2](#)) (Tang *et al.*, 2008). Systematic bias was corrected from non-redundant spectrum per peptide from all three search algorithms by using intensity normalization of protein quantification across samples by ProteoIQ2.7 (PREMIER Biosoft). Protein relative quantification was performed by using the ratios from tandem mass spectra when the peptides were uniquely assigned to detected protein. To be identified as being significantly differentially expressed, a protein had to be quantified with at least three peptides in experimental replicates, a *p* value <0.05, and a fold change >1.2 or <0.8 as determined with a Fisher's combined probability of <0.05 (Fisher, 1948). For identified proteins, the functional annotation was assigned to identified protein sequences by Blast2GO suite (Conesa *et al.*, 2005) (<http://www.blast2go.com/b2gome>) and confirmed with the Arabidopsis functional catalog (Bevan *et al.*, 1998). In addition, we used parametric analysis of gene set enrichment (PAGE) of the agriGO tool (<http://bioinfo.cau.edu.cn/agriGO>) to determine specifically enriched biological processes.

The proteomics data are available for public access at the PRIDE Archive–proteomics data repository (<http://www.ebi.ac.uk/pride/archive>). The MS proteomics data have been deposited to the ProteomeXchange Consortium (<http://proteomecentral.proteomexchange.org>) via the PRIDE partner repository (Vizcaino *et al.*, 2014) with the data-set identifier PXD001179 and DOI 10.6019/PXD001179.

## 2.5. Comparison of proteomic data with microarray data

The proteomics data were compared with a previous gene expression study (Paul *et al.*, 2013), which involved plants from the same experiment series on the ISS. In this comparison, we included 480 genes determined to be differentially

expressed at the transcript level from that study and 546 differentially expressed proteins from this study. Among them, 34 genes exhibited differential expression at both transcript and protein levels. To examine the degree of concordance between transcript and protein expression levels for those commonly differentially expressed genes, correlation tests for which Pearson's  $r$  and Spearman's  $\rho$  ( $r_s$ ) were used were conducted for a direct comparison of proteins and their corresponding transcript expression levels of those 34 genes using  $\log_2$ -fold change between ground and flight tissues. Those genes or proteins not differentially expressed at both the protein and transcript levels were not included in the correlation analysis.

## 2.6. Network analysis

The differentially abundant proteins were examined for cell wall associations by using SUBA3 searches (Tanz *et al.*, [2013](#)). The proteins returned with cell wall associations from SUBA3 were analyzed for interaction networking with GeneMANIA (Warde-Farley *et al.*, [2010](#)) with the Co-localization, Physical interactions, and Shared protein domains options, and Gene Ontology–based weighting.

## 3. Results

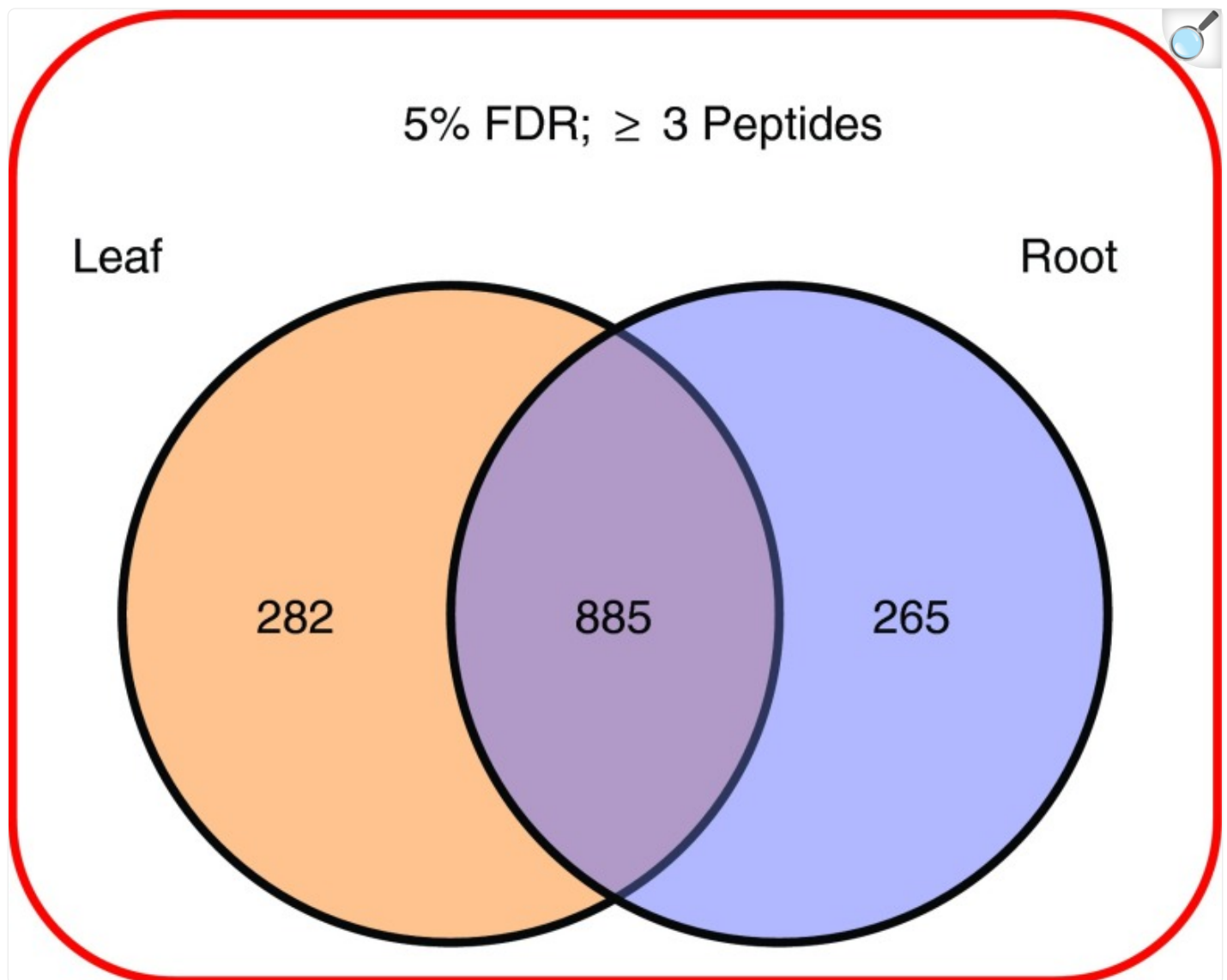
---

### 3.1. Protein recovery and identification in spaceflight material

RNAlater is widely used as an RNA preservative, primarily because it is a strong protein denaturant. Proteins can be recovered from RNAlater-preserved materials (van Eijnsden *et al.*, [2013](#)), but because the tissues and proteins are denatured, the biological properties of the subcellular components or proteins were not used to pre-separate proteins into classes such as soluble, cytoplasmic, membrane, or cell wall proteins. Therefore, the proteins identified in this study are simply considered soluble proteins according to the protocol used for their extraction. Sufficient protein was recovered from each sample to proceed with iTRAQ methods. Over 1500 proteins were identified in the root and leaf samples at a global FDR of 5% against the decoy database, and over 1300 proteins in each sample at an FDR of 1% (see [Supplementary Fig. S2](#)). An FDR of 5% was chosen as the cutoff for further analysis of proteins in this study.

Of the 1570 proteins identified in the samples at 5% FDR, 1167 leaf proteins and 1150 root proteins were identified with three or more protein-unique peptides, thus allowing them to be accurately quantified across the various flight and ground control samples ([Fig. 2](#)).

**FIG. 2.**



[Open in a new tab](#)

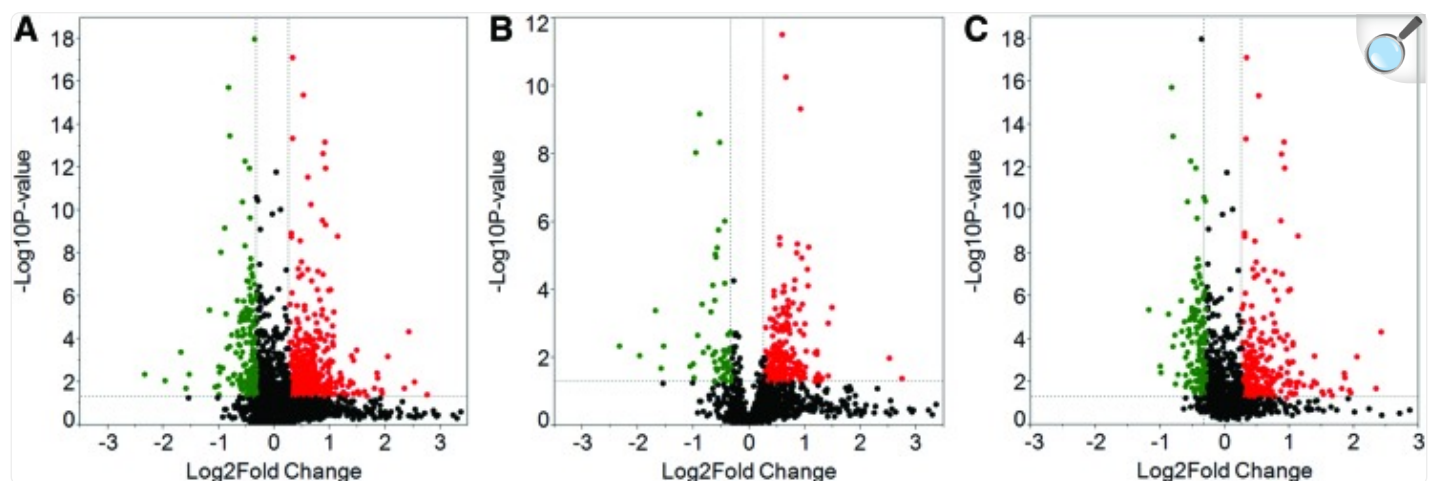
The number of proteins in the leaf and root samples meeting all the criteria for quantitation by iTRAQ. (Color graphics available online at [www.liebertonline.com/ast](http://www.liebertonline.com/ast) )

### 3.2. Differential protein abundance in spaceflight

A Fisher's test of combined probabilities was used to determine differences in quantitation values for each protein identified with three or more unique peptides. The Fisher's test accounted for the number of peptides identified in each

sample, together with the biological replicates of the root samples, to produce a  $p$  value for comparison of spaceflight versus ground controls for leaves and roots. Volcano plots of the  $p$  values and differential abundance as fold change of the root and leaf samples are presented in [Fig. 3](#). Currently, an iTRAQ method underestimates fold changes, implying small changes may indicate significant differences between samples (Bantscheff *et al.*, [2008](#); DeSouza *et al.*, [2009](#); Karp *et al.*, [2010](#)); thus, most iTRAQ studies use fold changes of  $<0.8$  or  $>1.2$ . Therefore, proteins were considered differentially abundant with  $p$  values greater than the threshold value ( $\alpha=0.05$ ) and fold-change values in excess of 0.8 and 1.2. [Figure 4](#) shows Venn diagrams of the number of proteins differing in abundance between spaceflight and ground control samples. Of the 1167 leaf proteins and 1150 root proteins that were able to be accurately quantified, 256 leaf proteins and 358 root proteins met the criteria of statistical significance by  $p$  value and differential abundance by fold change in the spaceflight samples. Only 41 of the significant differentially abundant proteins were shared between roots and leaves ([Fig. 4](#)).

### FIG. 3.

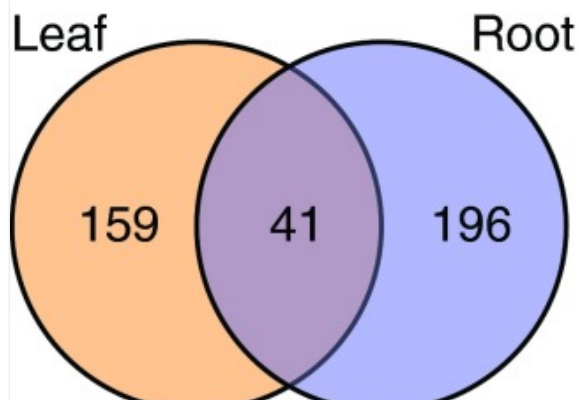
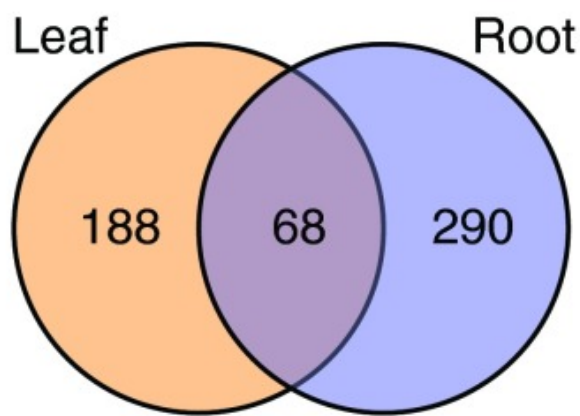


[Open in a new tab](#)

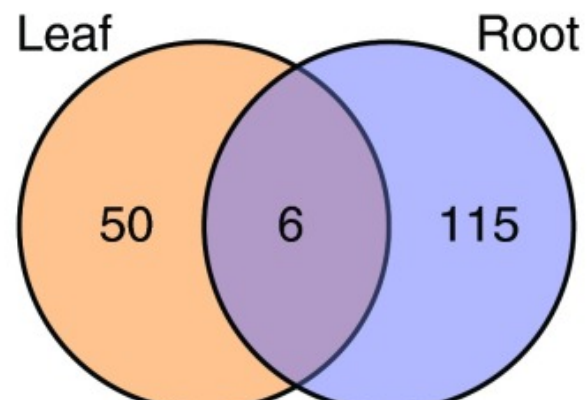
Volcano plots of differential expression between spaceflight and ground tissues. Negative  $\log_{10} p$  values were plotted on the  $y$  axis with log2 normalized fold change expression levels on the  $x$  axis. Significant differential expression with  $p$  value threshold values  $\alpha=0.05$  were present in areas exceeding the 0.8 and 1.2 of fold change threshold values. Red and green dots indicate up- and down-regulated protein in flight tissues relative to ground tissues. (A) Volcano plot for all proteins in either leaves or roots combined, (B) in leaves only, and (C) in roots only. (Color graphics available online at [www.liebertonline.com/ast](http://www.liebertonline.com/ast) )

**FIG. 4.**

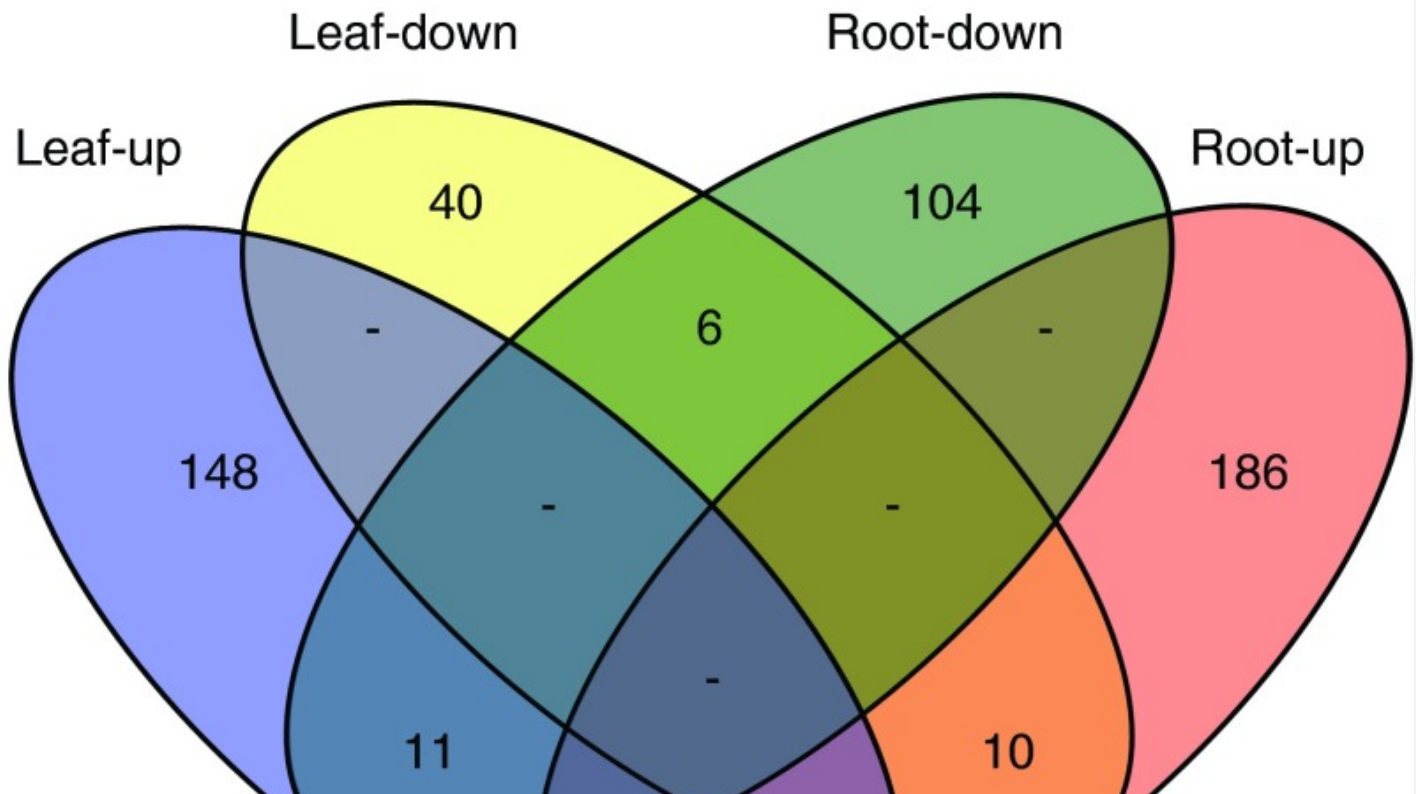
# Overall

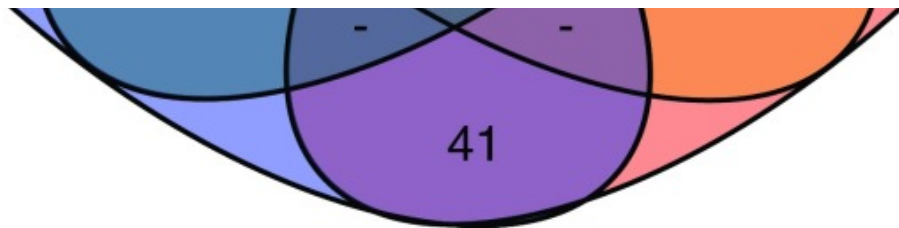


Up-regulation



Down-regulation



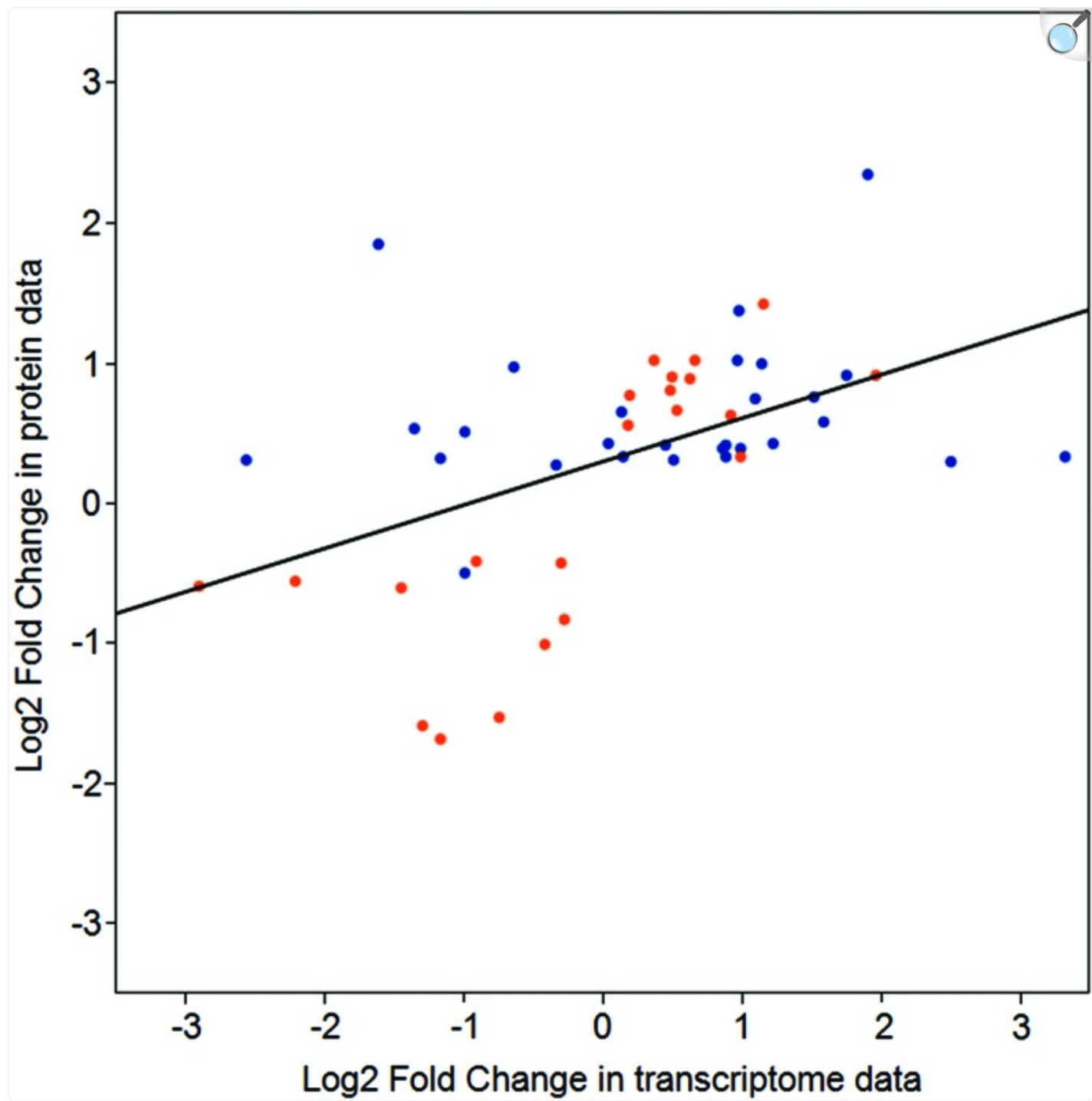


[Open in a new tab](#)

Summary of the differential protein accumulation in spaceflight samples compared to ground control. Overall, 358 root and 256 shoot proteins were differentially represented in the spaceflight sample. When parsed by whether the protein was increased or decreased in spaceflight, 237 root proteins and 200 shoot proteins were up-regulated and accumulated to more abundance in spaceflight, while 121 root proteins and 56 shoot proteins were down-regulated in spaceflight. (Color graphics available online at [www.liebertonline.com/ast](http://www.liebertonline.com/ast) )

In roots, 237 proteins were up-regulated in spaceflight, with an increase in abundance in the spaceflight samples meeting the significance criteria. In those same root samples, 121 proteins were found to be down-regulated and less abundant in spaceflight. For leaves, 200 proteins were more abundant in spaceflight, while 56 were less abundant. Again, few of these differentially regulated proteins were shared between the root and leaf samples. Only 47 proteins were similarly differentially abundant in both roots and leaves in spaceflight, being similarly increased or decreased in both tissues ([Fig. 5](#)). There were 21 proteins that were shared between roots and leaves but increased in one tissue and decreased in the other. A summary Venn diagram and table is presented at the bottom of [Fig. 4](#).

**FIG. 5.**



[Open in a new tab](#)

Comparison of gene and protein expression. Comparison of expression ratios from transcriptomic ( $x$  axis) and proteomic ( $y$  axis) profiling. Orange and blue dots indicate data from leaves and root tissue, respectively.  
(Color graphics available online at [www.liebertonline.com/ast](http://www.liebertonline.com/ast))

The 546 proteins that exhibited different abundances between spaceflight samples and the ground control samples are presented in [Table 1](#).

TABLE 1.

LIST AND PRIMARY ANNOTATIONS OF THE 546 PROTEINS SHOWN TO BE DIFFERENTIALLY ABUNDANT IN SPACEFLIGHT VERSUS GROUND CONTROLS IN THE COMBINED ARABIDOPSIS LINES OF THIS STUDY

Uniprot Accession no.	TAIR Accession	TAIR Annotation	Leaves FLT/GND Fold Change	Leaves FLT/GND p value	Roots FLT/GND Fold Change	Roots FLT/GND p value	Mazars
sp Q96292 ACT2_ARATH	AT3G18780.2	actin 2	0.779884	0.005664	0.702433	0.018658	0.533910
sp Q9LPW0 G3PA2_ARATH	AT1G12900.1	glyceraldehyde 3-phosphate dehydrogenase A subunit 2	0.726650	0.014196	0.607248	0.004562	
sp Q9E529 PURA_ARATH	AT3G57610.1	adenylosuccinate synthase	0.735619	0.015424	0.768180	0.020717	
sp P83291 NB5R2_ARATH	AT5G20080.1	FAD/NAD(P)-binding oxidoreductase	0.762217	0.014232	0.741374	0.000000	
sp Q80585 MTTHR2_ARATH	AT2G44160.1	methylenetetrahydrofolate reductase 2	0.600106	0.005124	0.697499	0.000010	
sp Q95IV5 RS2S1_ARATH	AT2G16360.1	Ribosomal protein S2S family	0.344880	0.004665	0.709730	0.003078	
tr Q9ZV55 Q9ZV55_ARATH	AT1G03230.1	Eukaryotic aspartyl protease family	1.595050	0.000879	0.798321	0.032081	
sp Q8LAH7 OPR1_ARATH	AT1G76680.1	12-oxophytodienoate reductase 1	1.550337	0.000113	0.692148	0.009421	
tr Q8LB85 Q8LB85_ARATH	AT5G04740.1	ACT domain-containing protein	1.351568	0.007869	0.657069	0.004953	
sp Q9FE58 RL223_ARATH	AT5G27770.1	Ribosomal L2e protein family	1.367938	0.007872	0.793272	0.025413	
sp Q9LV33 BG1L44_ARATH	AT3G18080.1	B-S glucosidase 44	1.383274	0.004556	0.742718	0.020136	
sp Q9ZUC1 QORL_ARATH	AT1G23740.1	Oxidoreductase, zinc-binding dehydrogenase family	1.568434	0.031665	0.781502	0.000000	
tr Q93ZET Q93ZET_ARATH	AT3G25000.1	Eukaryotic aspartyl protease family	1.635578	0.000339	0.734295	0.000000	
sp Q95K27 ENL1_ARATH	AT2G25060.1	early nodulin-like protein 14	1.427503	0.007232	0.725492	0.000007	
tr Q9SZ1 Q9SZ1_ARATH	AT4G31840.1	early nodulin-like protein 15	1.461443	0.008159	0.765427	0.000000	
sp Q95G54 CDSP_ARATH	AT1G76080.1	chloroplastic drought-induced stress protein of 32 kD	1.886642	0.001675	0.764496	0.000503	0.556240
sp Q9LW57 PAP6_ARATH	AT3G23400.1	Plastid-lipid associated protein PAP / fibrillin family	1.542774	0.013584	0.795352	0.001734	1.479800
sp Q9S2N1 VATB2_ARATH	AT4G38510.5	ATPase, V1 complex, subunit B protein	1.001400	0.995085	1.770334	0.005462	
sp Q9KEE2 ANX02_ARATH	AT5G65020.1	annexin 2	1.178449	0.243913	1.359553	0.024432	
sp Q23654 VATA_ARATH	AT1G78900.2	vacuolar ATP synthase subunit A	0.803510	0.019307	1.299405	0.019166	
sp Q43735 PER27_ARATH	AT3G01190.1	Peroxidase superfamily	1.010210	0.932163	1.207123	0.034169	
sp Q23044 PER3_ARATH	AT1G05260.1	Peroxidase superfamily	0.859908	0.142998	1.392846	0.044096	
sp Q9LF62 DAPF_ARATH	AT3G53580.1	diaminopimelate epimerase family	1.034066	0.863880	1.269726	0.026091	
tr Q95ZD6 Q95ZD6_ARATH	AT4G29060.1	elongation factor Ts family	0.908217	0.392524	1.242131	0.009183	
sp Q9F156 CLPC1_ARATH	AT5G50920.1	CLPC homologue 1	0.908765	0.370165	1.878057	0.026720	
sp P49200 RS201_ARATH	AT5G62300.2	Ribosomal protein S10p/S20e family	3.514292	0.072265	3.506316	0.020803	
sp Q3ECS3 BG1L35_ARATH	AT1G51470.1	beta glucosidase 35	1.113331	0.179777	1.237449	0.029423	
sp Q9SLF7 RLA22_ARATH	AT2G27710.3	60S acidic ribosomal protein family	1.183254	0.382376	1.703880	0.045652	
sp Q94AR8 LEUC_ARATH	AT4G13430.1	isopropyl malate isomerase large subunit 1	0.908488	0.663215	1.631117	0.031157	
sp Q8GRX1 BG1L34_ARATH	AT1G47600.1	beta glucosidase 34	1.135556	0.185083	1.392351	0.012343	
sp Q9FM01 UGDH4_ARATH	AT5G39320.1	UDP-glucose 6-dehydrogenase family	0.844533	0.147932	1.222161	0.000003	
sp Q95VMB R8G2_ARATH	AT4G13850.1	glycine-rich RNA-binding protein 2	2.188677	0.261170	1.473690	0.000136	
sp Q9SE60 MTTHR1_ARATH	AT3G59970.3	methylenetetrahydrofolate reductase 1	0.792237	0.144720	1.473690	0.000136	
sp Q9ZT4 GLNB_ARATH	AT4G01900.1	GLNB1 homolog	1.939772	0.259045	1.257022	0.030619	
sp Q49299 PGMC1_ARATH	AT1G23190.1	Phosphoglucomutase/phosphomannomutase family	0.916372	0.377632	1.820411	0.005276	
sp Q9STY6 RS202_ARATH	AT3G47370.3	Ribosomal protein S10p/S20e family	2.635398	0.087299	1.326032	0.004636	
sp Q9LXG1 RS91_ARATH	AT5G15200.1	Ribosomal protein S4	1.031297	0.857975	1.763175	0.000002	
tr Q9LV19 Q9LV19_ARATH	AT3G17810.1	pyrimidine 1	1.097072	0.305872	1.255289	0.000000	
sp P31168 COR47_ARATH	AT1G20440.1	cold-regulated 47	1.544321	0.353096	1.332902	0.002618	

tr O49607 O49607_ARATH	AT4G34980.1	subtilisin-like serine protease 2	1.184890	0.225550	1.840151	0.000000
sp Q43725 CYSKM_ARATH	AT3G59760.3	O-acetylserine (thiol) lyase isoform C	1.125392	0.178325	1.959433	0.003810
sp Q42521 DCE1_ARATH	AT5G17330.1	glutamate decarboxylase	0.880883	0.537648	1.284130	0.003242
sp P25864 RK9_ARATH	AT3G44890.1	ribosomal protein L9	1.146710	0.205937	2.023316	0.000001
sp Q42553 DI2_ARATH	AT3G02780.1	isopentenyl pyrophosphate:dimethylallyl pyrophosphate isomerase 2	1.089356	0.543635	1.741281	0.000044
tr Q501F7 Q501F7_ARATH	AT1G21401.1	Phosphoenolpyruvate carboxylase family	1.206318	0.392540	5.349830	0.000047
sp Q9M0Y8 NSF_ARATH	AT4G04910.1	AAA-type ATPase family	1.423873	0.522868	1.274094	0.010855
sp P48006 EF1D1_ARATH	AT1G30230.1	Glutathione S-transferase; Translation elongation factor EF1B	1.308152	0.053391	1.523805	0.028659
tr Q93V74 Q93V74_ARATH	AT4G34180.1	Cyclase family	1.684076	0.081240	1.248012	0.006148
sp P45724 PAL2_ARATH	AT3G53260.1	phenylalanine ammonia-lyase 2	0.729567	0.063507	1.383288	0.000000
sp Q8RWNP ODP22_ARATH	AT3G13930.1	Dihydrodippeptide acetyltransferase, long form protein	1.094891	0.445929	1.518556	0.000000
sp Q9C900 SOT16_ARATH	AT1G74100.1	sulfotransferase 16	0.951541	0.788685	3.632398	0.006606
sp Q9A4Z4 CML13_ARATH	AT1G12310.1	Calcium-binding EF-hand family	1.320450	0.076657	1.659180	0.000007
sp O82399 MDHg2_ARATH	AT2G22780.1	peroxisomal NAD-malate dehydrogenase 1	1.246866	0.107535	2.842764	0.028030
sp Q9FKW6 FNR1L_ARATH	AT5G66190.1	ferredoxin-NADP(+)-oxidoreductase 1	0.822970	0.293058	1.217404	0.000152
sp Q8V219 RL302_ARATH	AT1G77940.1	Ribosomal protein L7Ae/L30e/S12e/Gadd45 family	1.063128	0.582210	1.281420	0.011569
sp P59230 R10A2_ARATH	AT2G27530.2	Ribosomal protein L1p/L10e family	1.001342	0.993816	1.266453	0.021229
tr ABMRX2 ABMRX2_ARATH	AT5G18380.2	Ribosomal protein S5 domain 2-like superfamily	1.050151	0.615174	1.351650	0.030008
sp Q9C8F7 RL301_ARATH	AT1G36240.1	Ribosomal protein L7Ae/L30e/S12e/Gadd45 family	0.975498	0.708609	1.367699	0.000000
sp Q9T018 MTN1_ARATH	AT4G38800.1	methylthioadenosine nucleosidase 1	1.206560	0.414395	1.723382	0.000000
sp Q597L9 CX6B1_ARATH	AT1G24501.1	cytochrome C oxidase 6B	1.286145		1.387019	0.018129
sp Q9C5R8 BAS1B_ARATH	AT5G06290.1	2-cysteine peroxiredoxin B	0.887324	0.169052	1.386449	0.016755
tr Q0WP0U Q0WP0U_ARATH	AT2G17630.1	Pyridoxal phosphate (PLP)-dependent transferases superfamily	1.202398	0.156578	1.319039	0.000886
tr F4JTKB F4JTKB_ARATH	AT4G38220.2	Peptidase M20/M25/M40 family	0.862688	0.150675	1.418841	0.028244
sp Q9FFED RRAA2_ARATH	AT5G16450.2	Ribonuclease E inhibitor RraA/RNase_E_inh/diMeMenaQ_MeTrfase	1.535878	0.058260	1.703531	0.000019
sp Q9SEU6 TRXM4_ARATH	AT3G15360.1	thioredoxin M-type 4	2.240297	0.381917	1.491073	0.038645
sp Q9L206 GSTL3_ARATH	AT5G02790.1	Glutathione S-transferase family	1.194492	0.104814	1.692845	0.000045
sp Q92U83 SPD1_ARATH	AT1G23820.1	spermidine synthase 1	0.964483	0.906331	1.355015	0.000756
tr Q95ZM2 Q95ZM2_ARATH	AT4G38220.1	Peptidase M20/M25/M40 family	0.881214	0.214366	1.948043	0.000296
sp Q8L7R2 KHSE_ARATH	AT2G17265.1	homoserine kinase	1.542991		1.846414	0.000000
sp Q6IC28 NAC3_ARATH	AT5G13850.1	nascent polypeptide-associated complex subunit alpha-like protein 3	1.198352	0.098883	1.209030	0.001622
sp P14671 TRPB1_ARATH	AT5G65480.1	tryptophan synthase beta-subunit 1	1.117486	0.180304	1.676172	0.003328
sp Q92UT9 R5S1_ARATH	AT2G37270.2	ribosomal protein S8	0.958471	0.602481	1.295681	0.000425
sp P50061 RKA1_ARATH	AT1G07320.4	ribosomal protein L4	1.109009	0.736920	3.077478	0.027733
sp Q9F162 GLPQ1_ARATH	AT5G655480.1	SHIV3-like 1	1.107350	0.574594	1.372977	0.000033
sp Q95I81 FLAT2_ARATH	AT2G04780.2	FASCICLIN-like arabino-galactan 7	1.276552	0.334475	2.077867	0.000153
sp Q49506 GLO5_ARATH	AT4G18360.2	Aldolase-type TIM barrel family	0.654865	0.238783	1.390318	0.023065
sp Q95I20 EF1D2_ARATH	AT2G18110.1	Translation elongation factor EF1B/ribosomal protein S6 family	1.241976	0.320140	1.248551	0.000577
sp P93031 GMD2_ARATH	AT3G51160.1	NAD(P)-binding Rossmann-fold superfamily	0.812790	0.082088	1.493948	0.039404
sp Q9MBR8 RRAAA1_ARATH	AT3G02770.1	Ribonuclease E inhibitor RraA/RNase_E_inh/diMeMenaQ_MeTrfase	1.034192	0.942635	4.119772	0.000671
sp O24616 PSA7B_ARATH	AT5G66140.1	proteasome alpha subunit D2	1.225792	0.300650	1.559368	0.003248
tr Q95R74 Q95R74_ARATH	AT3G07320.1	O-Glycosyl hydrolases family 17 protein	1.152186	0.258487	1.297604	0.000794
tr F4IZE4 F4IZE4_ARATH	AT3G56310.2	Mellibiase family	1.463953	0.280449	1.295928	0.048503
tr F4JWF6 F4JWF6_ARATH	AT5G11200.2	DEAD/DEAH box RNA helicase family	1.170275	0.454617	1.209103	0.011613
sp Q8L027 PSB6_ARATH	AT4G31300.3	N-terminal nucleophile aminohydrolases [Ntn hydrolases] superfamily	1.158511	0.125385	1.570462	0.000948

sp Q96262 PCAP1_ARATH	AT4G20260.4	plasma-membrane associated cation-binding protein 1	1.220360	0.338307	1.665435	0.008688	0.735420
sp Q8H166 ALEU_ARATH	AT5G60360.1	aleurain-like protease	1.869481	0.298358	1.640443	0.000106	
tr Q94K85 Q94K85_ARATH	AT4G01610.1	Cysteine proteinases superfamily	1.154293	0.252551	1.283438	0.040363	
tr F4JC86 F4JC86_ARATH	AT3G13235.3	ubiquitin family	1.438142	0.154693	1.384716	0.000394	
sp Q9F029 RL212_ARATH	AT1G57660.1	Translation protein SH3-like family	1.143119	0.381605	1.802224	0.000091	
sp Q9C9K3 PPFA2_ARATH	AT1G76550.1	Phosphofructokinase family	3.870369	0.337813	1.514039	0.019081	
tr F4JPDB F4JPDB_ARATH	AT4G23895.3	Pleckstrin homology (PH) domain-containing protein	1.147265	0.318771	1.597493	0.021963	
sp P20115 CISY4_ARATH	AT2G44350.3	Citrate synthase family	0.948012	0.899771	1.589759	0.005818	
sp Q96299 14339_ARATH	AT2G42590.3	general regulatory factor 9	0.789873	0.078665	1.259101	0.005297	
tr O81493 O81493_ARATH	AT5G26260.1	TRAF-like family	1.507056	0.078782	1.267684	0.000835	
sp O22870 FK163_ARATH	AT2G43560.1	FKBP-like peptidyl-prolyl cis-trans isomerase family	1.081679	0.730780	1.409909	0.006675	
sp Q9L2X4 FLA10_ARATH	AT3G60900.1	FASCICLIN-like arabino-galactan-protein 10	6.229405	0.412893	1.518316	0.000011	
sp Q8LAD2 SUCA2_ARATH	AT5G23250.1	Succinyl-CoA ligase, alpha subunit	1.058172	0.070331	2.155033	0.018377	
sp Q56Z12 PATL2_ARATH	AT1G22530.1	PATELLIN 2	1.085025	0.719335	1.347213	0.001208	
sp Q43866 INV1_ARATH	AT3G13790.1	Glycosyl hydrolases family 32 protein	1.164912	0.427582	1.285115	0.003534	
sp O81235 SDOM1_ARATH	AT3G10920.1	manganese superoxide dismutase 1	1.615337		1.310110	0.000076	
sp Q9LMC9 GLT2_ARATH	AT1G18980.1	RmlC-like cupins superfamily	1.199751	0.677503	1.708032	0.000001	
tr O22581 O22581_ARATH	AT4G10750.1	Phosphoenolpyruvate carboxylase family	1.426045	0.520795	1.502989	0.006062	
tr Q8LE01 Q8LE01_ARATH	AT3G16850.3	Pectin lyase-like superfamily	1.696049		1.320333	0.000044	
tr Q80889 Q80889_ARATH	AT2G32520.1	alpha/beta-Hydrolases superfamily	1.203722	0.441790	1.220539	0.000017	
sp P43333 RU2A_ARATH	AT1G09760.3	U2 small nuclear ribonucleoprotein A	0.984956	0.944569	1.286783	0.033882	
sp Q84L30 RD230_ARATH	AT5G38470.1	Rad23 UV excision repair protein family	1.392029	0.251876	1.338474	0.001052	
tr OB2597 OB2597_ARATH	AT4G01480.1	pyrophosphorylase 5	1.407451	0.317046	1.253192	0.000141	
tr Q8LE79 Q8LE79_ARATH	AT3G60450.1	Phosphoglycerate mutase family	1.309989	0.447129	1.449623	0.000104	
sp Q95U13 FLA2_ARATH	AT4G12730.1	FASCICLIN-like arabino-galactan 2	1.353228	0.268451	1.311421	0.000536	
tr F4IA1X1 F4IA1X1_ARATH	AT1G31710.3	Copper amine oxidase family	1.401112	0.528732	2.014813	0.014285	
sp Q9FLP6 SU/M02_ARATH	AT5G55160.1	small ubiquitin-like modifier 2	1.557351	0.513923	1.348897	0.000379	
tr Q94B88 Q94B88_ARATH	AT3G17940.1	Galactose mutarotase-like superfamily	1.866989	0.387643	1.221877	0.023252	
sp Q95I75 EFGC_ARATH	AT1G62750.1	Translation elongation factor EFG/EFG2 protein	0.860109	0.363424	1.232760	0.006039	
tr Q94K56 Q94K56_ARATH	AT5G17710.1	Co-chaperone GrpE family	1.192782	0.225723	1.510285	0.044251	
sp Q22773 TL16_ARATH	AT4G02530.1	chloroplast thylakoid lumen protein	0.852872	0.300328	1.413918	0.024993	1.528700
sp Q42351 RL341_ARATH	AT1G26880.1	Ribosomal protein L34e superfamily	1.185908	0.426648	1.463441	0.035566	
sp Q9L5V0 GLYR1_ARATH	AT3G25530.2	glyoxylate reductase 1	1.006883	0.958721	2.276100	0.004012	
sp Q9C928 VATE2_ARATH	AT3G08560.1	vacuolar H+-ATPase subunit E isoform 2	1.106385	0.734776	1.344280	0.004937	
sp Q96330 FLS1_ARATH	AT5G08640.2	flavonol synthase 1	0.496664		1.827122	0.002386	
tr Q8V2G2 Q8V2G2_ARATH	AT3G50930.1	cytochrome BC1 synthesis	1.430454	0.122487	1.883917	0.000120	
tr Q9U13 Q9U13_ARATH	AT5G10160.1	Thioesterase superfamily	0.900719	0.446457	1.630504	0.005476	
sp Q9LD44 PER38_ARATH	AT4G08780.1	Peroxidase superfamily	0.749112	0.049380	1.249929	0.002118	
tr Q9ZVA1 Q9ZVA1_ARATH	AT1G78820.1	D-mannose binding lectin protein with Apple-like binding dom	0.496724	0.015544	2.022804	0.009989	
sp Q82663 SOHA1_ARATH	AT5G66760.1	succinate dehydrogenase 1-1	0.621893	0.000453	1.279746	0.019997	
sp Q8LG77 DH6_ARATH	AT3G09810.1	isocitrate dehydrogenase VI	0.739495	0.046574	1.521215	0.002356	
sp P42799 GS1_ARATH	AT5G63570.1	glutamate-1-semialdehyde-2,1-aminomutase	0.556086	0.000270	1.487912	0.002497	
sp Q42589 NLP1_ARATH	AT2G38540.1	lipid transfer protein 1	0.311048	0.000415	1.965453	0.001215	
sp Q9UL13 PREP1_ARATH	AT3G19170.1	presequence protease 1	0.769864	0.026823	1.333380	0.000003	
tr Q9ZUJ8 Q9ZUJ8_ARATH	AT2G15130.1	Plant basic secretory protein (BSP) family	0.333333	0.020940	1.242387	0.000000	

sp Q9LX29 ACR4_ARATH	AT3G59420.1	crinkly4	0.563711	0.007170	1.316849	0.000426
sp Q9LN0 PER8_ARATH	AT1G34510.1	Peroxidase superfamily	0.655770	0.006830	1.449629	0.002819
tr Q9LF98 Q9LF98_ARATH	AT3G52930.1	Aldolase superfamily	1.517016	0.000000	2.201513	0.000000
sp Q9SYT0 ANXD1_ARATH	AT1G35720.1	annexin 1	1.463679	0.000005	1.831470	0.000000
sp P46422 GSTF2_ARATH	AT4G02520.1	glutathione S-transferase PHI 2	2.803659	0.000334	1.884033	0.000000
sp Q9M9K1 PMG2_ARATH	AT3G08590.1	Phosphoglycerate mutase, 2,3-bisphosphoglycerate-independent	1.347727	0.001277	1.890009	0.013723
sp P42798 R15A1_ARATH	AT5G59850.1	Ribosomal protein S8 family	1.460963	0.000003	1.353814	0.000000
sp P49209 RL91_ARATH	AT1G3140.1	Ribosomal protein L6 family	1.774162	0.000053	1.415407	0.000000
sp P42794 R112_ARATH	AT4G24740.1	ribosomal protein large subunit 16A	1.252436	0.047340	1.216748	0.041342
tr Q8H788 Q8H788_ARATH	AT1G78830.1	Curculin-like (mannose-binding) lectin family	2.003559	0.039383	1.355172	0.017033
tr Q8L994 Q8L994_ARATH	AT3G18190.1	TCP-1/cpn60 chaperonin family	1.320378	0.009165	1.242674	0.007062
tr Q42105 Q42105_ARATH	AT1G07930.2	GTP binding Elongation factor Tu family	1.717120	0.009015	2.213190	0.010240
tr O65581 O65581_ARATH	AT4G26530.2	Aldolase superfamily	1.340110	0.041174	1.402473	0.000000
sp Q38936 FK152_ARATH	AT5G48580.1	FK506- and rapamycin-binding protein 15 kD-2	1.400098	0.000931	1.308217	0.039386
sp Q9LR2 LECT2_ARATH	AT3G15356.1	Legume lectin family	5.775426	0.010416	1.388039	0.019427
sp P16127 CHU1_ARATH	AT4G18480.1	P-loop containing nucleoside triphosphate hydrolases superfamily	1.444792	0.001613	1.629571	0.000753
tr Q9SAU2 Q9SAU2_ARATH	AT5G61410.2	D-ribulose-5-phosphate 3-epimerase	1.621701	0.001024	1.250210	0.001405
tr Q940G5 Q940G5_ARATH	AT4G25900.1	Galactose mutarotase-like superfamily	1.216808	0.011912	1.232660	0.009162
sp Q48646 GPX6_ARATH	AT4G11600.1	glutathione peroxidase 6	1.370120	0.020202	1.983269	0.000001
sp Q95E8U TRXM2_ARATH	AT4G03520.1	Thioredoxin superfamily	1.464840	0.020000	1.334792	0.000012
tr F4C591 F4C591_ARATH	AT1G12230.2	Aldolase superfamily	1.908744	0.024544	1.397617	0.006240
sp Q9CA59 NRP1_ARATH	AT1G74560.2	NAP1-related protein 1	1.262700	0.048228	1.485160	0.021579
sp Q95726 RPI3_ARATH	AT3G04790.1	Ribose 5-phosphate isomerase, type A protein	6.751234	0.040697	1.563486	0.000151
sp Q41931 ACCO2_ARATH	AT1G62380.1	ACCO oxidase 2	1.468037	0.018600	1.485523	0.000056
sp Q9FK25 OMT3_ARATH	AT5G54160.1	O-methyltransferase 1	1.696015	0.039712	1.259021	0.005250
tr Q8LC48 Q8LC48_ARATH	AT1G20580.1	Small nuclear ribonucleoprotein family	1.684242	0.039266	2.084047	0.000204
sp Q95VG4 RETOL_ARATH	AT4G20830.1	FAD-binding Berberine family	1.347114	0.005314	1.342190	0.000206
sp Q39099 XTH4_ARATH	AT2G06850.1	xyloglucan endotransglucosylase/hydrolase 4	2.013204	0.001032	2.153098	0.011175
tr Q9FF98 Q9FF98_ARATH	AT5G23820.1	MD-2-related lipid recognition domain-containing protein	1.564637	0.001461	1.347213	0.001208
sp Q94A97 UBC35_ARATH	AT1G78870.2	ubiquitin-conjugating enzyme 35	1.554395	0.039868	1.222315	0.024169
tr Q9CA69 Q9CA69_ARATH	AT1G14450.1	Protein of unknown function (DUF793)	2.031185	0.006532	1.225709	0.029464
tr F4J8V5 F4J8V5_ARATH	AT3G18770.1	Autophagy-related protein 13	1.580718	0.024737	1.421247	0.008963
tr F4KHA2 F4KHA2_ARATH	AT5G40170.1	receptor-like protein 54	1.858535	0.013652	1.329995	0.002488
sp Q95H76 PKM6_ARATH	AT2G07560.1	H(+)-ATPase 6	1.467210	0.013575	1.236961	0.000000
tr F4Y15 F4Y15_ARATH	AT5G41740.1	Disease resistance protein (TIR-NBS-LRR class) family	2.685392	0.035065	1.495242	0.000573
tr F4H83 F4H83_ARATH	AT1G35000.1	unknown protein	1.862053	0.018243	2.003271	0.032372
sp Q04203 HSPR2_ARATH	AT2G40000.1	ortholog of sugar beet HS1 PRO-1-2	1.749374	0.023675	5.083850	0.020225
tr F4I4A6 F4I4A6_ARATH	AT1G10300.1	Nucleolar GTP-binding protein	1.876731	0.045306	1.337276	0.005527
sp Q9LMR5 FK126_ARATH	AT1G15670.1	Galactose oxidase/kelch repeat superfamily	1.257500	0.039358	1.314272	0.006627
sp P50883 R1L21_ARATH	AT2G37390.1	Ribosomal protein L11 family	1.607263	0.000592	1.475292	0.000286
sp Q64879 BGL15_ARATH	AT2G44450.1	beta glucosidase 15	1.554558	0.023416	1.518006	0.040578
tr Q9V9Y1 Q9V9Y1_ARATH	AT4G10300.1	RmC-like cupins superfamily	2.020020	0.019418	2.080521	0.001141
tr F4BU0 F4BU0_ARATH	AT3G60440.1	Phosphoglycerate mutase family	2.478982	0.040217	1.244525	0.000001
sp Q95W09 R5101_ARATH	AT4G25740.1	RNA-binding Plectin/S10 domain-containing protein	0.929417	0.904413	1.431438	0.002864
sp Q04450 TCPE_ARATH	AT1G24510.1	TCP-1/cpn60 chaperonin family	0.822572	0.081001	1.234468	0.018188

sp Q9XFH8 TRXF1_ARATH	AT3G02730.1	thioredoxin F-type 1	1.518041	0.069583	1.299498	0.000204
sp P49206 RS261_ARATH	AT2G40590.1	Ribosomal protein S26e family	1.033822	0.800224	2.627737	0.000617
sp Q9LX12 INC3_ARATH	AT5G10170.1	myo-inositol-1-phosphate synthase 3	0.651870		1.496996	0.000123
sp Q96252 ATP4_ARATH	AT5G47030.1	ATPase, F1 complex, delta/epsilon subunit	0.865753	0.646498	1.596986	0.000000
tr Q8HOX9 Q8HOX9_ARATH	AT3G23570.1	alpha/beta-Hydrolases superfamily	1.188004		1.397477	0.017537
tr Q9SU04 Q9SU04_ARATH	AT4G23730.1	Galactose mutarotase-like superfamily	0.840360		1.308909	0.007332
tr Q8H7A6 Q8H7A6_ARATH	AT1G54410.1	dehydron family	0.998610		1.271622	0.025052
sp P46248 AATS_ARATH	AT4G31990.2	aspartate aminotransferase 5	1.249708	0.589999	1.385617	0.007008
sp Q95X16 CLPP3_ARATH	AT1G66670.1	CLP protease proteolytic subunit 3	1.726738		1.350315	0.000018
tr Q9M360 Q9M360_ARATH	AT3G61780.1	embryo defective 1703	1.670208	0.492587	2.594626	0.009903
sp Q9LUV2 POP3_ARATH	AT3G17210.1	heat stable protein 1	1.263017	0.610770	1.355261	0.004284
sp P92959 RK24_ARATH	AT5G54600.1	Translation protein SH3-like family	3.020504	0.391252	1.221690	0.000327
sp P35131 UBCB_ARATH	AT5G41700.4	ubiquitin conjugating enzyme 8	0.923464		1.678422	0.000194
tr Q949W8 Q949W8_ARATH	AT5G49650.1	xylulose kinase-2	1.029572	0.450775	1.225683	0.040617
sp Q82211 RUXG_ARATH	AT2G23930.1	probable small nuclear ribonucleoprotein G	1.606518		2.675869	0.012042
sp Q94CD8 E134_ARATH	AT3G13560.3	O-Glycosyl hydrolases family 17 protein	0.870850	0.279342	1.278091	0.008685
tr B9DHX7 B9DHX7_ARATH	AT3G52370.1	FASICLIN-like arabinogalactan protein 15 precursor	1.058502	0.821026	2.022852	0.005110
tr Q8L8T0 Q8L8T0_ARATH	AT5G62350.1	Plant invertase/pectin methylesterase inhibitor superfamily	1.809472	0.138649	1.747846	0.005990
sp Q9ZR03 UCRA_ARATH	AT4G03280.1	photosynthetic electron transfer C	0.642598	0.122537	1.359630	0.001692
tr Q94BY3 Q94BY3_ARATH	AT5G14030.4	stilicon-associated protein beta (TRAPb) family	1.332386		1.661961	0.026998
sp Q9AS56 CP20B_ARATH	AT5G13120.1	cyclophilin 20-2	18.409256		1.274757	0.049986
sp Q56WK6 PATL1_ARATH	AT1G72150.1	PATELLIN 1	1.384463	0.145750	1.639574	0.013637
sp Q42533 BCCP1_ARATH	AT5G16390.1	chloroplastic acetylcoenzyme A carboxylase 1	1.231671	0.252378	2.534103	0.016813
tr Q93Z34 Q93Z34_ARATH	AT2G24280.1	alpha/beta-Hydrolases superfamily	0.939871	0.921752	2.052053	0.033968
tr Q8GW53 Q8GW53_ARATH	AT4G24340.1	Phosphorylase superfamily	1.045165	0.904101	1.573716	0.019158
sp Q948K6 RABG1_ARATH	AT5G39620.1	RAB GTPase homolog G1	1.096049		2.134505	0.036320
sp Q9AV97 KDS41_ARATH	AT1G79500.4	Aldolase-type TIM barrel family	4.197914	0.402366	1.963443	0.009204
sp Q9LXAB BXL6_ARATH	AT5G10560.1	Glycosyl hydrolase family	1.135347	0.713071	1.288234	0.001797
sp P43296 RD19A_ARATH	AT4G39090.1	Papain family cysteine protease	0.985405	0.477321	1.527393	0.039267
sp Q9CE83 TPS26_ARATH	AT2G66020.1	Terpenoid cyclases/Protein prenyltransferases superfamily	0.645247		1.256120	0.005182
sp Q858Q7 P1P183_ARATH	AT2G34370.1	Pentatricopeptide repeat (PPR) superfamily	0.715285	0.575171	1.259840	0.028065
tr Q9SNB6 Q9SNB6_ARATH	AT3G46620.1	zinc finger [C3H4-type RING finger] family	1.391546	0.260100	1.696001	0.009359
tr Q8LA4J Q8LA4J_ARATH	AT5G57950.1	26S proteasome regulatory subunit, putative	0.746074		2.327771	0.014279
sp Q95IV0 SUR1_ARATH	AT2G20610.1	Tyrosine transaminase family	0.972243	0.758675	1.398509	0.000786
sp Q9LF3 GASE_ARATH	AT5G14920.1	Gibberellin-regulated family	7.667009		1.265005	0.025092
sp Q94AW8 DNAJ3_ARATH	AT3G44110.1	DNAJ homolog 3	0.667655	0.365397	1.476417	0.033633
tr Q8LE12 Q8LE12_ARATH	AT5G58070.1	temperature-induced lipocalin	1.282092	0.173774	1.376432	0.019450
sp Q8L831 NUDT3_ARATH	AT1G79690.1	nudix hydrolase homolog 3	5.552230	0.404207	1.327669	0.006376
sp Q8LFH7 RL371_ARATH	AT1G15250.1	Zinc-binding ribosomal protein family	1.508948	0.349781	1.531460	0.039690
sp Q49629 PAP2_ARATH	AT4G22440.1	Plastid-lipid associated protein PAP/fibrillin family	1.138663	0.774263	1.614947	0.023992
tr Q9SX53 Q9SX53_ARATH	AT1G50380.1	Prokaryotic peptidase family	0.455949		1.951753	0.000066
sp Q8L7K9 MAO2_ARATH	AT4G05070.1	NAD-dependent malic enzyme 2	1.213979		1.419989	0.015864
tr F4I2M6 F4I2M6_ARATH	AT1G09890.1	Rhamnogalacturonate lyase family	1.151005	0.318500	1.261859	0.000000
sp Q96329 ACOX4_ARATH	AT3G51840.1	acyl-CoA oxidase 4	0.545552		1.556586	0.010262
sp Q95X68 RK1B_ARATH	AT1G48350.1	Ribosomal L18p/L5e family	1.778382	0.354679	1.366810	0.004620

sp Q9FGH9 E70B1_ARATH	AT5G58430.1	exocyst subunit exo70 family B1	1.680509	0.083932	1.349678	0.001008
tr F4JHV8 F4JHV8_ARATH	AT4G02840.2	Small nuclear ribonucleoprotein family	1.616070		1.482634	0.027595
tr QBGZ20 QBGZ20_ARATH	AT5G67310.1	cytochrome P450, family 81, subfamily G, polypeptide 1	1.378982	0.164953	1.684580	0.007033
sp Q9ZQ97 U73C4_ARATH	AT2G36770.1	UDP-Glycosyltransferase superfamily	1.390123	0.225234	1.772189	0.004302
sp Q9MAJ7 B6A5L5_ARATH	AT1G45130.3	beta-galactosidase 5	0.614876		1.417210	0.001263
tr O65538 O65538_ARATH	AT4G32605.1	Mitochondrial glycoprotein family	0.587495		1.336061	0.020324
tr Q9SSB7 Q9SSB7_ARATH	AT1G80240.1	Protein of unknown function, DUF642	0.851612		1.557130	0.004199
tr O65655 O65655_ARATH	AT4G39680.2	SAP domain-containing protein	1.371160	0.507757	1.442850	0.000000
tr Q8RWPO Q8RWPO_ARATH	AT3G20790.1	NAD(P)-binding Rossmann-fold superfamily	1.153702		1.467106	0.000652
tr O64595 O64595_ARATH	AT1G70410.3	beta carbonic anhydrase 4	1.006101		1.261193	0.005373
sp O80477 MES3_ARATH	AT2G23610.1	methyl esterase 3	1.178343	0.354271	1.354365	0.031918
sp Q9XFS7 NLTPS_ARATH	AT3G51600.1	lipid transfer protein 5	2.016845		1.412937	0.002349
tr QBLT79 TH04B_ARATH	AT5G02530.2	RNA-binding (RRM/RBD/RNP motifs) family	1.424225		1.290423	0.026422
sp Q43387 PER71_ARATH	AT5G64120.1	Peroxidase superfamily	0.940678	0.842869	1.574671	0.002834
tr Q9SNE4 Q9SNE4_ARATH	AT3G50230.1	Leucine-rich repeat protein kinase family	1.376847	0.472876	3.807606	0.024387
sp Q9FMU6 MPCP3_ARATH	AT5G614040.1	phosphate transporter 3;1	1.118557		3.851190	0.034052
tr Q8LP54 Q8LP54_ARATH	AT3G06670.1	binding	22.107592		1.472073	0.026663
sp Q9FZD4 PPRS9_ARATH	AT1G26500.1	Pentatricopeptide repeat (PPR) superfamily	1.234966		2.073834	0.038615
sp Q8GV8E CAPP4_ARATH	AT1G68750.1	phosphoenolpyruvate carboxylase 4	0.832394		1.989744	0.001436
tr Q9M216 Q9M216_ARATH	AT3G58300.1	Arabidopsis phospholipase-like protein (PEARLI 4) family	0.343044	0.057190	3.600255	0.003936
tr Q9WM57 Q9WM57_ARATH	AT5G08670.1	ATP synthase alpha/beta family	1.076187	0.314517	1.898868	0.000000
sp Q9CAI7 IF4A3_ARATH	AT1G72730.1	DEA(D/H)-box RNA helicase family	0.683397	0.305406	1.606949	0.037433
tr O23722 O23722_ARATH	AT2G38700.1	mevalonate diphosphate decarboxylase 1	1.696058	0.088749	3.174942	0.044580
sp Q8LC68 NRP2_ARATH	AT1G18800.1	NAP1-related protein 2	1.664429	0.055673	1.602307	0.013429
tr Q9V556 Q9V556_ARATH	AT1G01050.1	pyrophosphorylase 1	2.242864	0.362942	1.480498	0.016493
sp Q9RS55 RAA5B_ARATH	AT3G07410.1	RAB GTPase homolog A5B	1.570724	0.067235	1.358005	0.000361
tr F4IKB3 F4IKB3_ARATH	AT2G16230.1	O-Glycosyl hydrolases family 17 protein	1.161233	0.015090	1.488287	0.021840
sp Q9SRZ4 PRX2C_ARATH	AT1G65970.1	thioredoxin-dependent peroxidase 2	1.359777		1.489916	0.017891
tr F4KGDS F4KGDS_ARATH	AT5G58830.1	Subtilisin-like serine endopeptidase family	1.073818	0.547337	1.208656	0.000004
sp Q95II0 H2AV2_ARATH	AT2G38810.1	histone H2A.8	2.048568	0.099666	1.520694	0.020016
tr Q9SUN5 Q9SUN5_ARATH	AT4G20440.1	small nuclear ribonucleoprotein associated protein B	2.400421	0.184755	1.485667	0.003198
tr Q9LV3M3 Q9LV3M3_ARATH	AT5G58250.3	unknown protein	1.321327	0.197745	1.632479	0.012023
sp Q9STL4 CEP2_ARATH	AT3G48340.1	Cysteine proteinases superfamily			1.694703	0.042559
sp Q84LG4 COP2_ARATH	AT3G09800.1	SNARE-like superfamily	1.502102	0.086344	1.330882	0.013465
sp Q9LZB8 Y5370_ARATH	AT5G03700.1	D-mannose binding lectin protein with Apple-like binding dom	1.761554	0.225660	2.888649	0.037160
sp Q9RSV5 METE2_ARATH	AT3G03780.3	methionine synthase 2	0.923647	0.740046	0.674208	0.010524
sp P93047 HMG83_ARATH	AT1G20696.2	high mobility group B3	4.753242	0.427406	0.748724	0.001011
sp O82662 SUCB_ARATH	AT2G20420.1	ATP citrate lyase (ACL) family	1.235570	0.325566	0.782103	0.023920
sp Q9FF58 R5102_ARATH	AT5G641520.1	RNA binding Plectin/S10 domain-containing protein	0.753667	0.552591	0.789590	0.004855
sp Q9FY64 R5154_ARATH	AT5G09510.1	Ribosomal protein S19 family	1.060300	0.682430	0.499785	0.001934
sp Q9L266 SIR_ARATH	AT5G04590.1	sulfite reductase	0.978866	0.816518	0.592001	0.012687
sp P51407 R1A21_ARATH	AT2G27720.1	60S acidic ribosomal protein family	1.307520	0.141498	0.443826	0.000005
sp Q9URR9 GLO1_ARATH	AT3G14420.2	Aldolase-type TIM barrel family	2.976482	0.314410	0.749260	0.010344
tr O04496 O04496_ARATH	AT1G09750.1	Eukaryotic aspartyl protease family	1.855033	0.139825	0.574497	0.000226
sp Q93WJ8 MDAR4_ARATH	AT5G03630.1	Pyridine nucleotide-disulfide oxidoreductase family	1.034899	0.841011	0.681869	0.001739

tr F4JW99 F4JW99_ARATH	AT5G04430.2	binding to TOMV RNA 1L (long form)	1.184829	0.197003	0.729306	0.022346
sp O24457 ODPA3_ARATH	AT1G01090.1	pyruvate dehydrogenase E1 alpha	1.170864	0.064426	0.698943	0.001541
sp Q9CL84 ETHE1_ARATH	AT1G53580.1	glyoxalase II 3	1.161230	0.574219	0.789588	0.014238
sp O04983 ACCC_ARATH	AT5G35360.1	Acetyl Co-enzyme a carboxylase biotin carboxylase subunit	0.906886	0.342762	0.769990	0.005968
sp Q9SSK7 MLP34_ARATH	AT1G70850.3	MLP-like protein 34	1.045699	0.655369	0.783628	0.036768
sp Q96266 GSTFB_ARATH	AT2G47730.1	glutathione S-transferase phi 8	1.311070	0.069112	0.759644	0.002845
sp P43082 HEVL_ARATH	AT3G04720.1	pathogenesis-related 4	2.502072	0.250914	0.695734	0.000000
sp Q8VZH2 APM1_ARATH	AT4G33090.1	aminopeptidase M1	0.873013	0.111968	0.748195	0.000000
sp Q9V309 SCP45_ARATH	AT1G28130.2	serine carboxypeptidase-like 4S	1.160849	0.067420	0.651210	0.000016
sp Q9LQL0 GC5H3_ARATH	AT1G32470.1	Single hybrid motif superfamily	0.796207	0.142986	0.759464	0.000000
sp Q38814 THI4_ARATH	AT5G54770.1	thiazole biosynthetic enzyme, chloroplast [ARA6] (THI1) (THI4)	2.672115	0.551250	0.572389	0.000000
sp Q95K23 R5122_ARATH	AT2G32060.3	Ribosomal protein L7Ae/L30e/S12e/Gadd45 family	1.400240	0.056341	0.762877	0.000949
sp Q91Q08 ATPG1_ARATH	AT4G04640.1	ATPase, F1 complex, gamma subunit protein	0.966171	0.477638	0.791984	0.000010
sp Q9C891 DIR20_ARATH	AT1G55210.2	Disease resistance-responsive (dirigent-like protein) family	1.114636	0.252814	0.758651	0.000000
sp Q680A5 KPR54_ARATH	AT2G42910.1	Phosphoribosyltransferase family	0.920058		0.565377	0.000000
sp P31167 ADT1_ARATH	AT3G08580.2	ADP/ATP carrier 1	0.811421	0.147666	0.789469	0.000001
tr Q9ZW84 LEUD1_ARATH	AT2G43100.1	isopropylmalate isomerase 2	1.204476	0.315728	0.798835	0.000001
sp Q8HY10 ODPA2_ARATH	AT1G24180.1	Thiamin diphosphate-binding fold (THDP-binding) superfamily	1.055736	0.618267	0.747068	0.008758
sp P41916 RAN1_ARATH	AT5G20010.1	RAS-related nuclear protein-1	1.066847	0.660398	0.779427	0.000000
sp P42759 ERD10_ARATH	AT1G20450.3	Dehydrin family	1.390275		0.725927	0.000000
tr Q9LTQ5 Q9LTQ5_ARATH	AT3G20370.1	TRAF-like family	1.370956	0.406554	0.738421	0.000000
sp P94111 STS1_ARATH	AT1G74020.1	strictosidine synthase 2	1.178546	0.125294	0.798858	0.032138
sp Q22914 CP121_ARATH	AT2G47400.1	CP12 domain-containing protein 1	1.108403		0.787991	0.000022
tr O64767 O64767_ARATH	AT2G35040.1	AIACRF1/IMPCHase bimenzoyl family	0.493736	0.057075	0.775524	0.000164
sp Q94X9 NACA2_ARATH	AT3G49470.3	nascent polypeptide-associated complex subunit alpha-like protein 2	0.185607		0.757301	0.000181
tr Q9F2K4 Q9FK4_ARATH	AT1G27310.1	nuclear transport factor 2A	1.587049	0.104578	0.797553	0.001354
sp Q9CS14 R571_ARATH	AT1G48830.2	Ribosomal protein S2e family	1.908752	0.080131	0.762323	0.007647
tr Q9FIX1 Q9FIX1_ARATH	AT5G39730.1	ANG-like (avirulence induced gene) family	1.322538	0.078177	0.799055	0.005325
sp Q8L756 HEX03_ARATH	AT1G65590.1	beta-hexosaminidase 3	0.793456	0.345124	0.739747	0.000031
sp Q8RXU5 R37A2_ARATH	AT3G60245.1	Zinc-binding ribosomal protein family	2.046481	0.329026	0.771694	0.000443
tr Q8WJ3 Q8WV3_ARATH	AT4G29690.1	Alkaline-phosphatase-like family	1.127197	0.637843	0.712465	0.000000
sp Q949X7 DCDA1_ARATH	AT3G14390.1	Pyridoxal-dependent decarboxylase family	0.996514	0.985863	0.751364	0.000029
tr F4JM51 F4JM51_ARATH	AT4G28940.1	Phosphorylase superfamily	0.882957		0.771752	0.000840
sp O23717 PSB5A_ARATH	AT1G13060.1	20S proteasome beta subunit E1	0.537753	0.197896	0.764001	0.000016
sp Q9CSU3 PR58A_ARATH	AT5G19990.1	regulatory particle triple-A ATPase 6A	3.753221	0.438836	0.783949	0.000096
tr Q1H595 Q1H595_ARATH	AT1G03330.1	Small nuclear ribonucleoprotein family	1.104486	0.395214	0.737774	0.000000
sp Q9C820 RAG3D_ARATH	AT1G52280.1	RAB GTPase homolog G30	0.998236	0.994354	0.755808	0.000002
sp P92995 GLT1_ARATH	AT1G18970.1	germin-like protein 4	1.536775	0.365339	0.668451	0.012158
tr Q9LN5 Q9LN5_ARATH	AT1G20225.1	Thioredoxin superfamily	1.481863	0.366699	0.747120	0.000002
sp P55217 METB_ARATH	AT3G01120.3	Pyridoxal phosphate [PLP]-dependent transferases superfamily	0.896161		0.629149	0.000002
tr Q9L5T0 Q9L5T0_ARATH	AT5G60160.1	Zn-dependent exopeptidases superfamily	0.812695	0.221746	0.735208	0.000004
sp Q9CP16 AIM1_ARATH	AT4G29010.1	Enoyl-CoA hydratase/isomerase family	0.848778	0.470081	0.796536	0.000095
sp P47924 RIBA1_ARATH	AT5G64300.1	GTP cyclohydrolase II	1.838134	0.180150	0.706090	0.000004
sp O80517 BCB2_ARATH	AT2G44790.1	uclacyanin 2	4.047497	0.496997	0.732265	0.000008
tr Q8L1AN3 P4H4_ARATH	AT5G18900.1	2-oxoglutarate (2OG) and Fe(III)-dependent oxygenase superfamily	1.008774	0.921424	0.720697	0.000007

sp Q9UR30 GGT1_ARATH	AT1G23310.2	glutamate:glyoxylate aminotransferase	0.940311	0.593490	0.774285	0.000081
sp Q9FLX7 NDUJ5_ARATH	AT5G52840.1	NADH-ubiquinone oxidoreductase-related	1.412140	0.092483	0.749260	0.010344
sp Q9FVE6 HDT1_ARATH	AT3G44750.3	histone deacetylase 3	1.692352	0.190257	0.707062	0.003625
tr F4JVN6 TPPII_ARATH	AT4G20850.1	tripeptidyl peptidase ii	1.233421	0.261395	0.705469	0.000145
sp Q9M669 E137_ARATH	AT4G34480.1	O-Glycosyl hydrolases family 17 protein	0.900960	0.019057	0.679957	0.000036
sp P41088 CF1_ARATH	AT3G55120.1	Chalcone-flavanone isomerase family	0.712331		0.793536	0.005943
tr QBLZM6 Q9LZMB_ARATH	AT5G02050.1	Mitochondrial glycoprotein family	1.347871	0.393519	0.673688	0.000000
tr Q9LPZ1 Q9LPZ1_ARATH	AT1G14301.1	plastid developmental protein DAG, putative	0.890313		0.798414	0.002868
sp Q9FXA2 PABP_ARATH	AT1G49760.2	poly(A) binding protein 8	1.091101	0.534362	0.740530	0.000053
sp Q9C667 CPNB4_ARATH	AT1G26230.2	TCP-1/cpn60 chaperonin family	1.070427	0.805962	0.545798	0.000007
sp Q9CA23 UFM1_ARATH	AT1G77710.1	Ubiquitin-like, Ufm1	1.230727	0.732998	0.789869	0.000356
tr O65220 O6522D_ARATH	AT5G35100.1	Cyclophilin-like peptidyl-prolyl cis-trans isomerase family	1.236153	0.051873	0.756641	0.000005
sp Q9AC59 PATL4_ARATH	AT1G30690.2	Sec14p-like phosphatidylinositol transfer family			0.759186	0.000541
tr QBLFM3 QBLFM3_ARATH	AT5G66920.1	SKUS similar 17	0.987041		0.690696	0.000060
tr Q42028 Q42028_ARATH	AT4G01700.1	Chitinase family	0.926432		0.782727	0.019602
tr Q5M314 Q9M314_ARATH	AT3G61540.1	alpha/beta-Hydrolases superfamily	1.109825	0.129145	0.687633	0.000013
sp Q9FJK3 VDAC2_ARATH	AT5G67500.1	voltage-dependent anion channel 2	0.926341	0.750779	0.749185	0.002469
tr Q9LFX8 Q9LFX8_ARATH	AT1G27090.1	glycine-rich protein	0.889027		0.632532	0.000046
sp Q9FP14 RAD2B_ARATH	AT5G47200.1	RAB GTPase homolog 1A			0.779881	0.003439
tr O81835 O81835_ARATH	AT4G27320.1	Adenine nucleotide alpha hydrolases-like superfamily	0.957106	0.212276	0.791583	0.025305
sp Q9FG34 PER54_ARATH	AT5G06730.1	Peroxidase superfamily	2.270287		0.787463	0.009083
tr Q949M6 Q949M6_ARATH	AT1G55040.1	zinc finger (Ran-binding) family	1.450357		0.791843	0.006514
tr Q94AT6 Q94AT6_ARATH	AT3G04000.1	NAD(P)-binding Rossmann-fold superfamily	1.068485		0.674909	0.000077
sp Q9Z2H0 LYM1_ARATH	AT1G21880.1	Iym domain GPI-anchored protein 1 precursor	1.277714		0.772231	0.029215
sp Q9ZNT1 NB5R1_ARATH	AT5G17700.1	NADH:cytochrome B5 reductase 1	1.618081		0.736104	0.009343
tr F4I5H7 F4I5H7_ARATH	AT1G70570.2	anthranilate phosphoribosyltransferase, putative	1.173545	0.790690	0.782997	0.000911
sp Q9SLN5 MAP1A_ARATH	AT2G45240.1	methionine aminopeptidase 1A	0.932197	0.845718	0.704476	0.000005
sp Q9LSJ2 AB2B2_ARATH	AT3G28415.1	ABC transporter family	1.500299	0.311341	0.787123	0.001103
sp Q9FNNS NDUV1_ARATH	AT5G08530.1	51 kDa subunit of complex I	1.373496		0.723264	0.000013
tr Q9VC3 Q9VC3_ARATH	AT2G41380.1	S-adenosyl-L-methionine-dependent methyltransferases superfamily	1.029663		0.726464	0.004303
tr A8MRP2 A8MRP2_ARATH	AT2G42940.1	AGL2-like (avirulence induced gene) family	1.295350		0.759884	0.004191
sp Q39102 FTSH1_ARATH	AT1G50250.1	FTSH protease 1	1.608076	0.217746	0.752645	0.004233
sp Q9C6B3 GCA2_ARATH	AT1G47260.1	gamma carbonic anhydrase 2	1.434314		0.656581	0.000708
tr Q9LK22 Q9LK22_ARATH	AT3G27310.2	plant UBX domain-containing protein 1	1.792723		0.586733	0.000065
sp Q8LD49 TRXK_ARATH	AT1G50320.1	thioredoxin X	1.399953	0.349823	0.782396	0.004323
sp POCB23 Y4862_ARATH	AT4G38070.1	basic helix-loop-helix (bHLH) DNA-binding superfamily	0.982847		0.505628	0.003705
sp Q39214 RPM1_ARATH	AT3G07040.1	NB-ARC domain-containing disease resistance protein	0.937582		0.780096	0.023353
tr Q9LMQ2 Q9LMQ2_ARATH	AT1G15820.1	light-harvesting complex photosystem II subunit 6	0.172399		0.657119	0.016568
tr Q8UKA4 UBA2C_ARATH	AT3G15010.2	RNA-binding (RRM/RBD/RNP motifs) family	7.588067		0.776326	0.019569
tr Q9Z51 Q9Z51_ARATH	AT3G16190.1	Isochorismatase family	1.151395		0.641510	0.000189
sp O80575 RIS8_ARATH	AT2G44050.1	6,7-dimethyl-8-ribityllumazine synthase / riboflavin synthase	0.626723		0.787123	0.012081
tr B9DFH3 B9DFH3_ARATH	AT5G55920.1	S-adenosyl-L-methionine-dependent methyltransferases superfamily	0.928772		0.673268	0.000409
tr Q9S205 Q9S205_ARATH	AT4G29830.1	Transducin/WD40 repeat-like superfamily	2.443573		0.779463	0.035535
sp P52032 GPX1_ARATH	AT2G25080.1	glutathione peroxidase 1	1.505170		0.724941	0.031450
sp Q9M153 GDL61_ARATH	AT4G01130.1	GDSL-like Lipase/Acylhydrolase superfamily	0.837771	0.836333	0.753030	0.000136

tr Q93W05 Q93W05_ARATH	AT1G10590.2	Nucleic acid-binding, OB-fold-like protein	1.665011		0.795506	0.009017
sp Q93VR3 GME_ARATH	AT5G28840.2	GDP-D-mannose 3',5'-epimerase	0.921611		0.766073	0.000327
sp Q95795 BADH1_ARATH	AT1G74920.1	aldehyde dehydrogenase 10A8	1.018438		0.794217	0.001443
sp Q9WV25 TBA4_ARATH	AT1G04820.1	tubulin alpha-4 chain	1.185514	0.212177	0.786686	0.001162
sp Q95R37 BG123_ARATH	AT3G09260.1	Glycosyl hydrolase superfamily	1.518166	0.026961		
tr Q9SJQ9 Q9SJQ9_ARATH	AT2G36460.1	Aldolase superfamily	1.522253	0.000117		2.072100
sp PODH99 EF1A1_ARATH	AT5G60390.3	GTP-binding Elongation factor Tu family	1.363244	0.000155		
tr F4KS89 F4KS89_ARATH	AT5G07030.1	Eukaryotic aspartyl protease family	1.552469	0.000076		
sp Q08682 R5SA1_ARATH	AT1G27370.2	40S ribosomal protein SA	1.305823	0.000731		
sp P23686 METK1_ARATH	AT1G02500.2	S-adenosylmethionine synthetase 1	1.380639	0.004192		
sp Q95N86 MDHP_ARATH	AT3G47520.1	malate dehydrogenase	1.570050	0.001521		
sp Q9SMU8 PER34_ARATH	AT3G49120.1	peroxidase CB	1.463169	0.003377		7.313600
sp P17562 METK2_ARATH	AT4G01850.2	S-adenosylmethionine synthetase 2	1.362347	0.013266		
sp Q93VG5 R5B1_ARATH	AT5G20900.1	Ribosomal protein S8e family	1.437880	0.000589		
sp P60040 RL72_ARATH	AT2G01250.1	Ribosomal protein L30/L7 family	1.381065	0.010556		
sp Q95IL8 METK3_ARATH	AT2G36880.2	methionine adenosyltransferase 3	1.276409	0.007486		
sp Q92VF3 ML328_ARATH	AT2G01520.1	MLP-like protein 328	1.362242	0.035124		
sp Q9LUT2 METK4_ARATH	AT3G17390.1	S-adenosylmethionine synthetase family	1.481445	0.006105		
sp O80852 GSTF9_ARATH	AT2G30860.1	glutathione S-transferase PHI 9	1.319765	0.013537		1.794500
tr B9DFJ0 B9DFJ0_ARATH	AT3G51800.3	metalloleptotidase M24 family	1.237427	0.011186		
sp P60039 RL73_ARATH	AT2G44120.1	Ribosomal protein L30/L7 family	1.244369	0.038765		
sp O04314 PYBP1_ARATH	AT3G16420.3	PKY10-binding protein 1	1.304071	0.048658		
sp Q9XFT3 PSBQ1_ARATH	AT4G21280.1	photosystem II subunit QA	1.757441	0.000098		
sp Q8VYK6 R5A3_ARATH	AT5G58420.1	Ribosomal protein S4 (RPS4A) family	1.298300	0.017000		
tr Q95URO Q95URO_ARATH	AT4G23670.1	Polyketide cyclase/dehydrase and lipid transport superfamily	1.801382	0.021137		
sp P49204 R5A2_ARATH	AT5G07090.1	Ribosomal protein S4 (RPS4A) family	1.306104	0.020345		
sp Q49006 PME3_ARATH	AT3G14310.1	pectin methylesterase 3	1.368348	0.004440	0.763280	0.080598
sp Q9MSK2 DLDH2_ARATH	AT3G17240.3	lipoamide dehydrogenase 2	1.441257	0.027275		
tr Q9ZVA4 Q9ZVA4_ARATH	AT1G78850.1	D-mannose binding lectin protein with Apple-like binding dom	1.658111	0.000582		
tr Q9LSQ5 Q9LSQ5_ARATH	AT5G54500.1	flavodoxin-like quinone reductase 1	1.284209	0.022352		
sp Q93251 R8G8_ARATH	AT4G39260.1	cold, circadian rhythm, and RNA binding 1	1.257112	0.007421		
sp P51414 RL261_ARATH	AT3G49910.1	Translation protein SH3-like family	1.232190	0.006415		
sp Q8W4HB GDL19_ARATH	AT1G54010.1	GDSL-like Lipase/Acylhydrolase superfamily	1.867289	0.000382		
sp Q42403 TRXH3_ARATH	AT5G42980.1	thioredoxin 3	1.452207	0.033889		
sp Q957H1 PSAD1_ARATH	AT4G02770.1	photosystem I subunit D-1	2.105650	0.000006		
sp Q38931 FKB62_ARATH	AT3G25230.1	rotamase FKBP 1	1.452394	0.010576		
sp P34788 R518_ARATH	AT1G34030.1	Ribosomal protein S13/S18 family	1.655802	0.001957	1.056116	0.114741
sp P24101 PER33_ARATH	AT3G49110.1	peroxidase CA	1.339055	0.000760		
sp Q9FWR4 DHAR1_ARATH	AT1G19570.1	dehydroascorbate reductase	1.827236	0.032961		
sp Q42262 R53A2_ARATH	AT4G34670.1	Ribosomal protein S3Ae	1.809271	0.000008		
tr Q95FB1 Q95FB1_ARATH	AT3G08030.1	Protein of unknown function, DUF642	1.511640	0.008734		
sp Q9CAVD R53A1_ARATH	AT3G04840.1	Ribosomal protein S3Ae	1.829061	0.000004		
sp Q95112 ATP7_ARATH	AT2G21870.1	copper ion binding; cobalt ion binding; zinc ion binding	1.270756	0.008801		
sp Q95A56 PSAD2_ARATH	AT1G03130.1	photosystem I subunit D-2	2.105650	0.000006		
sp P41127 RL131_ARATH	AT3G49010.3	breast basic conserved 1	2.690952	0.000996	1.934218	0.203585

sp Q9FVQ1 NUCL1_ARATH	AT1G48920.1	nucleolin-like 1	1.403990	0.004800		1.781000
sp Q95IHO RS141_ARATH	AT2G36160.1	Ribosomal protein S11 family	1.263615	0.026693		
sp Q95F40 RL4A_ARATH	AT3G09630.1	Ribosomal protein L4/L1 family	1.456765	0.005906		
tr Q8W4G8 Q8W4G8_ARATH	AT5G03690.2	Aldolase superfamily	1.594452	0.000476		2.406600
sp P49691 RL4B_ARATH	AT5G02870.1	Ribosomal protein L4/L1 family	1.408852	0.028904	1.131630	0.465307
sp Q9CAK6 RS142_ARATH	AT3G11510.1	Ribosomal protein S11 family	1.245625	0.024411		
sp P59232 R27AB_ARATH	AT2G47110.2	ubiquitin 6	1.299603	0.041064		
tr QDWMP6 QDWMP6_ARATH	AT3G20390.1	endoribonuclease L-PSP family	1.350200	0.038563		
tr F4JT64 F4JT64_ARATH	AT4G19410.2	Pectinacetyl esterase family	1.626328	0.000210		
sp Q95GA6 RS191_ARATH	AT3G02080.1	Ribosomal protein S19e family	1.511701	0.004307		
sp P42036 RS143_ARATH	AT3G52580.1	Ribosomal protein S11 family	1.224901	0.026805		
sp Q80934 Y2766_ARATH	AT2G37660.1	NAD(P)-binding Rossmann-fold superfamily	2.446613	0.046120		
sp Q9LX88 R15A4_ARATH	AT3G46404.1	ribosomal protein S15A-D	1.299256	0.018858		
sp Q94080 RL183_ARATH	AT5G27850.1	Ribosomal protein L18e/L15 superfamily	1.325029	0.017190		
sp P42761 GSTFA_ARATH	AT2G30870.1	glutathione S-transferase PHI 10	1.255481	0.044821		
sp Q39242 TRXB2_ARATH	AT2G17420.1	NADPH-dependent thioredoxin reductase A	1.283611	0.040269		
sp P46283 S17P_ARATH	AT3G55800.1	sedoheptulose-bisphosphatase	1.227091	0.001337	3.324041	0.207564
sp Q9LZ9H RL182_ARATH	AT3G62870.1	Ribosomal protein L7Ae/L30e/S12e/Gadd45 family	1.588259	0.000000	1.160833	0.000000
sp P42791 RL182_ARATH	AT3G05590.1	ribosomal protein L18	1.378665	0.012969	0.895306	0.030229
tr Q92UF6 Q92UF6_ARATH	AT2G05920.1	Subtilase family	1.298331	0.037869		
sp Q95UT2 PER39_ARATH	AT4G11290.1	Peroxidase superfamily	1.897269	0.016393		
tr Q94F20 Q94F20_ARATH	AT5G25460.1	Protein of unknown function, DUF642	2.294650	0.039131	0.975884	0.070777
tr Q6KFR8 Q6KFR8_ARATH	AT5G03240.3	polyubiquitin 3	1.518456	0.000347	0.941488	0.011158
sp QBLJG3 ESM1_ARATH	AT3G14210.1	epithiospecific modifier 1	1.586931	0.007141	0.844697	0.159895
sp Q93V13 RL171_ARATH	AT1G27400.1	Ribosomal protein L22p/L17 family	1.607309	0.008774		
tr F4HW16 F4HW16_ARATH	AT1G28290.2	arabinogalactan protein 31	1.398056	0.001463	5.385590	0.371962
sp P49692 RL7A1_ARATH	AT2G47610.1	Ribosomal protein L7Ae/L30e/S12e/Gadd45 family	1.366611	0.000110		
sp Q95MT7 4CLLA_ARATH	AT3G48990.1	AMP-dependent synthetase and ligase family	1.520031	0.031475	0.777179	0.254513
tr Q8LDQ7 Q8LDQ7_ARATH	AT5G47210.1	Hyaluronan/mRNA-binding family	1.454485	0.007278		
tr Q9AEZ7 Q9AEZ7_ARATH	AT1G63000.1	nucleotide-rhamnose synthase/epimerase-reductase	1.319774	0.031841		
sp Q38900 CP19A_ARATH	AT2G16600.1	ratemase CYP 3	1.323235	0.021269	1.079585	0.146976
sp Q95S31 PSA1_ARATH	AT4G28750.1	Photosystem I reaction center subunit IV/PsaE protein	1.924361	0.000012		
sp Q9LF30 RS192_ARATH	AT5G15520.1	Ribosomal protein S19e family	1.488807	0.008852	0.872151	0.145330
sp Q3E7K8 UBCQ12_ARATH	AT1G50603.1	ubiquitin 12	1.482036	0.001175	0.842172	0.166692
tr Q9LJM9 Q9LJM9_ARATH	AT3G26460.1	Polyketide cyclase/dehydrase and lipid transport superfamily	1.213153	0.035113	0.733246	0.053893
sp Q9FHQ6 UBQ9_ARATH	AT5G37640.1	ubiquitin 9	1.402233	0.007168		
sp Q8LD03 RS73_ARATH	AT5G16130.1	Ribosomal protein S7e family	1.526330	0.000496		
sp Q39258 VATE1_ARATH	AT4G11150.1	vacuolar ATP synthase subunit E1	1.519185	0.007423	6.530557	0.292772
sp P51413 RL172_ARATH	AT1G67430.1	Ribosomal protein L22p/L17 family	1.647452	0.010255		
tr Q8LCM9 Q8LCM9_ARATH	AT5G11420.1	Protein of unknown function, DUF642	2.385645	0.041943	1.108662	0.223373
tr Q92VA5 Q92VA5_ARATH	AT1G78860.1	D-mannose binding lectin protein with Apple-like binding dom	1.608725	0.011272	1.027329	0.345723
tr Q8W112 Q8W112_ARATH	AT5G20950.2	Glycosyl hydrolase family	1.427399	0.008746	0.830302	0.035173
sp Q96518 PER16_ARATH	AT2G18980.1	Peroxidase superfamily	1.381955	0.036168	1.046502	0.219624
sp Q95T14 PSAE2_ARATH	AT2G20260.1	photosystem I subunit E-2	1.949541	0.000270	2.550920	0.191023
sp Q95R73 RS281_ARATH	AT5G03850.1	Nucleic acid-binding, OB-fold-like protein	2.088711	0.000078	1.058291	0.000873
sp Q95CK3 EF1B2_ARATH	AT5G19510.1	Translation elongation factor EF1B/ribosomal protein S6 family	1.508596	0.001360		3.447600
sp Q95K39 SBP3_ARATH	AT2G24940.1	membrane-associated progesterone binding protein 2	1.616199	0.000308		
sp Q95L8A8 FABI_ARATH	AT2G05990.2	NAD(P)-binding Rossmann-fold superfamily	1.244632	0.020540	0.912405	0.249302
sp Q95GZ5 BXL7_ARATH	AT1G78060.1	Glycosyl hydrolase family	1.421074	0.011324		
tr Q8LB8A3 Q8LB8A3_ARATH	AT4G35630.1	phosphoserine aminotransferase	1.347253	0.002269	0.883672	0.041524
tr F4JH10 F4JH10_ARATH	AT4G02450.2	HSP20-like chaperones superfamily	1.381146	0.021521		
sp Q9LRX8 R13A2_ARATH	AT3G24830.1	Ribosomal protein L13 family	1.586737	0.003420	1.481184	0.055184
tr Q8LAE9 Q8LAE9_ARATH	AT5G45280.2	Pectinacetyl esterase family	1.555965	0.011475		
tr Q42214 Q42214_ARATH	AT4G05050.3	ubiquitin 11	1.455947	0.005374	0.971363	0.051626
sp Q95P91 RS121_ARATH	AT1G15930.2	Ribosomal protein L7Ae/L30e/S12e/Gadd45 family	1.342053	0.039138	1.037446	0.053838
sp P17745 EF1U_ARATH	AT4G20360.1	RAB GTPase homolog E1B	1.383985	0.000371	0.990691	0.000147
tr Q8L790 Q8L790_ARATH	AT1G76160.1	SKUS similar 5	1.526977	0.001614	1.239384	0.130807
sp Q8GYB8 OPR2_ARATH	AT1G76690.1	12-oxophytodienoate reductase 2	1.427176	0.007391	1.084781	0.001174
sp O65351 SUB1_ARATH	AT5G67360.1	Subtilase family	1.297098	0.007495	2.208163	0.089080
sp Q38935 FK151_ARATH	AT3G25220.1	Fk506-binding protein 15 kD-1	1.392000	0.044467	1.051282	0.001518
sp P49690 RL23_ARATH	AT3G04400.1	Ribosomal protein L14p/L23e family	2.076138	0.000026	0.974378	0.000000
sp Q8LER3 XTH17_ARATH	AT4G37800.1	xyloglucan endotransglucosylase/hydrolase 7	1.721130	0.000248	1.118475	0.013466
sp Q42342 CYB5A_ARATH	AT5G53560.1	cytochrome B5 isoform E	1.389713	0.019525	0.908505	0.000392
sp O04905 KCY3_ARATH	AT5G26667.3	P-loop containing nucleoside triphosphate hydrolases superfamily	1.386302	0.011660	0.937371	0.000363
sp Q9T791 EFITM_ARATH	AT4G02930.3	GTP-binding Elongation factor Tu family	1.308562	0.033716	0.810730	0.000087
sp Q5XF33 CHIL2_ARATH	AT5G45930.1	magnesium chelatase i2	1.496572	0.047426	0.956915	0.000881
sp P52577 IFRH_ARATH	AT1G75280.1	NMR-like negative transcriptional regulator family	1.247525	0.028577	1.032576	0.420968
tr Q9FZ47 Q9FZ47_ARATH	AT1G16880.1	uridylyltransferase-related	1.545249	0.043872	0.810114	0.000050
sp Q9M352 RL362_ARATH	AT3G53740.1	Ribosomal protein L36e family	1.756039	0.007611	0.856486	0.002164
sp Q9FGY1 BX1_ARATH	AT5G49360.1	beta-xylosidase 1	2.324971	0.007934	1.143776	0.001757
tr Q8GU4 Q8GU4_ARATH	AT4G21650.1	Subtilase family	2.275574	0.007423	0.869913	0.001373
tr Q9FKU8 Q9FKU8_ARATH	AT5G44400.1	FAD-binding Berberine family	1.269914	0.037875	1.076816	0.011865
sp O22160 TL15A_ARATH	AT2G44920.2	Tetratricopeptide repeat (TPR)-like superfamily	1.488496	0.043780	0.983890	0.003187
sp Q95ES0 BG118_ARATH	AT1G52400.2	beta glucosidase 18	1.633405	0.001096	0.909922	0.006181
sp Q9LZ57 RL363_ARATH	AT5G02450.1	Ribosomal protein L36e family	1.736049	0.029956	1.029485	0.380171
sp Q95F53 RL351_ARATH	AT3G09500.1	Ribosomal L29 family	1.928135	0.036681	1.068402	0.002426
sp O04922 GPX2_ARATH	AT2G31570.1	glutathione peroxidase 2	1.333638	0.037405	1.291171	0.075301
sp Q8GW78 CLP41_ARATH	AT4G12060.1	Double Clp-N motif protein	1.762421	0.014463	1.105458	0.005151
sp O81126 RZP22_ARATH	AT4G31580.2	serine/arginine-rich 22	1.581136	0.048852	0.848769	0.053649
sp Q84TFO AKRCA_ARATH	AT2G37790.1	NAD(P)-linked oxidoreductase superfamily	1.512319	0.027440	1.146808	0.017496
sp Q9E533 ADHX_ARATH	AT5G43940.1	GroES-like zinc-binding dehydrogenase family	1.641735	0.020443	0.921729	0.064487
tr O65660 O65660_ARATH	AT4G39730.1	Lipase/lipoxygenase, PLAT/LH2 family	1.262895	0.022118	1.000362	0.000042
sp Q9L241 RL354_ARATH	AT5G02610.1	Ribosomal L29 family	1.988633	0.027775	1.103714	0.025808
sp Q9M770 PRX2F_ARATH	AT3G06050.1	peroxiredoxin IIF	1.521161	0.026183	1.079920	0.289348
sp Q9ZUR7 ARG1_ARATH	AT2G37500.2	arginine biosynthesis protein Arg1 family	1.707544	0.005407	0.820513	0.000055
sp Q9FF8 MD368_ARATH	AT5G52470.1	fibrillarin 1	1.852009	0.025100	2.471371	0.083624
sp Q9FLQ4 DOO2A_ARATH	AT5G55070.1	Dihydrofolate reductase/succinyltransferase	1.447069	0.035064	1.581961	0.069916
sp Q94AH9 MD36A_ARATH	AT4G25630.1	fibrillarin 2	1.778661	0.001028	0.837270	0.001674
sp P42731 PABP2_ARATH	AT4G34110.1	poly(A) binding protein 2	1.307106	0.021986	1.188685	0.003827
sp Q9LNN2 LECT3_ARATH	AT1G53070.1	Legume lectin family	1.434412	0.011854	0.833651	0.009094

sp Q9T029 R5254_ARATH	AT4G39200.1	Ribosomal protein S25 family	2.366889	0.030734	0.921327	0.011474
sp O64644 SAP18_ARATH	AT2G45640.1	SIN3 associated polypeptide P18	1.518639	0.001148		
sp Q3E8E5 BGL3B_ARATH	AT5G48375.1	thioglucoside glucosidase 3	2.323648	0.006499	3.128846	0.145124
tr Q9LVRS Q9LVRS_ARATH	AT5G66650.1	Protein of unknown function (DUF607)	2.031185	0.006532	3.139868	0.257926
tr Q57XV5 Q57XV5_ARATH	AT4G24350.1	Phosphorylase superfamily	1.971741	0.002123	1.424760	0.063842
tr Q9SJ01 Q9SJ01_ARATH	AT2G42760.1	unknown protein	1.700383	0.021606	3.751976	0.062461
tr F4IXX3 F4IXX3_ARATH	AT3G49400.1	Transducin/WD40 repeat-like superfamily	1.541660	0.017720	1.082549	0.242637
sp Q9SL42 PIN1_ARATH	AT2G18040.1	peptidylprolyl cis/trans isomerase, NIMA-interacting 1	1.589908	0.022958	1.060635	0.200621
sp Q9C912 R3SA3_ARATH	AT1G74270.1	Ribosomal protein L35Ae family	1.294876	0.038949	0.818148	0.005204
sp Q8VWG7 TDX_ARATH	AT3G17880.2	tetratricopeptide domain-containing thioredoxin	1.449631	0.035605	0.966059	0.227626
sp Q8L3K9 KASM_ARATH	AT2G04540.1	Beta-ketoacyl synthase	1.262468	0.017819		
sp Q8GTY0 EF1AA_ARATH	AT1G07920.1	GTP-binding Elongation factor Tu family	1.894842	0.000000	1.115826	0.001595
sp P59223 R5131_ARATH	AT3G60770.1	Ribosomal protein S13/S15	1.356534	0.024806	0.973267	0.003835
sp P25269 TRBP2_ARATH	AT4G27070.1	tryptophan synthase beta-subunit 2	1.399478	0.034677	1.166284	0.055385
sp O64518 MCA5_ARATH	AT1G79330.1	metacaspase 5	1.677042	0.031548	1.148342	0.107061
sp Q9F2H0 R53A2_ARATH	AT1G41880.1	Ribosomal protein L35Ae family	1.668588	0.012981	1.052320	0.050980
sp P33157 E13A_ARATH	AT3G57260.1	beta-1,3-glucanase 2	1.426474	0.045127		
sp P19366 ATPB_ARATH	ATCG00480.1	ATP synthase subunit beta	0.737313	0.000001		
sp O23255 SAHH1_ARATH	AT4G13940.1	S-adenosyl-L-homocysteine hydrolase	0.738363	0.000065		
sp P53492 ACT7_ARATH	AT5G09810.1	actin 7	0.779557	0.006826		0.668700
sp Q8RWV0 TKTC1_ARATH	AT3G60750.1	Transketolase	0.692524	0.000000		
sp Q9LK36 SAHH2_ARATH	AT3G23810.1	S-adenosyl-L-homocysteine (SAH) hydrolase 2	0.790168	0.001794	0.948754	0.317446
sp Q9FFR3 6PGD2_ARATH	AT5G41670.2	6-phosphogluconate dehydrogenase family	0.773643	0.022376		
sp P10797 RBS2B_ARATH	AT5G38420.1	Ribulose bisphosphate carboxylase (small chain) family	0.662867	0.000011		
sp Q0WN25 METE3_ARATH	AT5G20980.2	methionine synthase 3	0.674299	0.000006		
sp P10795 RBS1A_ARATH	AT1G67090.1	ribulose bisphosphate carboxylase small chain 1A	0.537920	0.000000		
sp Q42560 AC01_ARATH	AT4G35830.1	acotinase 1	0.765669	0.02124		
sp P10796 RBS1B_ARATH	AT5G38430.1	Ribulose bisphosphate carboxylase (small chain) family	0.659118	0.000009		
sp P53496 ACT11_ARATH	AT3G12110.1	actin-11	0.680960	0.000002		
sp Q9SH69 6PGD1_ARATH	AT1G64190.1	6-phosphogluconate dehydrogenase family	0.736511	0.049340		
sp Q39161 NIR_ARATH	AT2G15620.1	nitrite reductase 1	0.705261	0.039516		
sp Q9AB78 GCSP1_ARATH	AT4G33010.1	glycine decarboxylase P-protein 1	0.514856	0.000000		0.441610
tr F4JB05 F4JB05_ARATH	AT3G12915.1	Ribosomal protein S5/Elongation factor G/III/V family	0.650103	0.000205		
sp P25856 G3PA1_ARATH	AT3G26650.1	glyceraldehyde 3-phosphate dehydrogenase A subunit	0.756767	0.018558		
sp Q9ZN27 GLTB1_ARATH	AT5G04140.2	glutamate synthase 1	0.635179	0.000073		
sp P56757 ATPA_ARATH	ATCG00120.1	ATP synthase subunit alpha	0.652343	0.049800	1.015132	0.207076
sp F4IW47 TKTC2_ARATH	AT2G45290.1	Transketolase	0.762398	0.006856		
sp P41376 F4A1_ARATH	AT3G13920.1	eukaryotic translation initiation factor 4A1	0.635484	0.008373	0.822602	0.195430
sp Q93ZN9 DAPAT_ARATH	AT4G33680.1	Pyridoxal phosphate (PLP)-dependent transferases superfamily	0.740302	0.006125		
sp Q38799 ODPB1_ARATH	AT5G50850.1	Transketolase family	0.735034	0.009178	0.807313	0.059180
tr Q9AK05 Q9AK05_ARATH	AT3G03960.1	TCP-1/cpn60 chaperonin family	0.759405	0.025513	0.918873	0.011822
sp P41377 F4A2_ARATH	AT1G54270.1	eif4a-2	0.650133	0.013695		
sp O80988 GCSP2_ARATH	AT2G26080.1	glycine decarboxylase P-protein 2	0.723005	0.019530	0.960137	0.126085
sp Q9LYA9 CP41A_ARATH	AT3G63140.1	chloroplast stem-loop binding protein of 41 kDa	0.767493	0.013262	0.831574	0.000000
sp P27140 CAHC_ARATH	AT3G01500.3	carbonic anhydrase 1	0.525557	0.002239	1.008109	0.127564
sp P25855 GC5H1_ARATH	AT2G35370.1	glycine decarboxylase complex H	0.735270	0.033535	1.060359	0.018594
sp Q9C9W5 HPR1_ARATH	AT1G68010.2	hydroxypyruvate reductase	0.728991	0.006325	1.165233	0.022242
sp Q43127 GLNA2_ARATH	AT5G35630.3	glutamine synthetase 2	0.699525	0.011342	0.863585	0.000050
sp P04778 CB1C_ARATH	AT1G29930.1	chlorophyll A/B binding protein 1	0.198641	0.004549	0.920775	0.055876
sp Q9LUKO PKP1_ARATH	AT3G22960.1	Pyruvate kinase family	0.574340	0.024295	0.950755	0.178665
sp P33154 PR1_ARATH	AT2G14610.1	pathogenesis-related gene 1	0.729624	0.048922	1.111132	0.036946
tr F4J2K4 F4J2K4_ARATH	AT3G10180.1	P-loop containing nucleoside triphosphate hydrolases superfamily	0.741665	0.043187	1.056612	0.020380
sp P13114 CHSY_ARATH	AT5G13930.1	Chalcone and stilbene synthase family	0.501615	0.040357	1.106382	0.012390
sp Q95AA6 PPR34_ARATH	AT1G11710.1	Pentatricopeptide repeat (PPR) superfamily	0.661559	0.021046	1.185975	0.114404
sp Q94AS2 RH2_ARATH	AT3G19760.1	eukaryotic initiation factor 4A-III	0.480130	0.017953	0.753921	0.073830
tr Q9FKE4 Q9FKE4_ARATH	AT5G45210.1	Disease resistance protein (TIR-NBS-LRR class) family	0.678791	0.021407	0.916156	0.148146
sp Q8V287 CB1B_ARATH	AT1G29910.1	chlorophyll A/B binding protein 3	0.256025	0.008713	1.377813	0.062409

[Open in a new tab](#)

Blank cells indicate that the protein was not present or did not meet quantitation criteria in that sample. Green cells indicate that the protein is more abundant in the spaceflight sample. Red cells indicate less abundant in spaceflight. Where directly correlated by TAIR annotation, the microgravity results from Mazars *et al.* (2014) are indicated in the last column.

Table 1 is available in color online at [www.liebertonline.com/ast](http://www.liebertonline.com/ast)

### 3.3. Functional analysis of proteins differentially abundant in spaceflight

When the proteomic changes were highlighted in global metabolic pathways (<http://pmn.plantcyc.org/overviewsWeb/>

[celOv.shtml?orgid=ARA](#) ), the effects of spaceflight were obviously different between leaf and root tissues ([Supplementary Fig. S3](#) and also referring elements of [Table 1](#)). In addition, PAGE showed quite distinct patterns between leaves and roots when comparing the differential abundance based on the functional classification of the proteins ([Table 2](#)). For example, responses to light stimulus and response to radiation were similar, as were pathways involving cell wall metabolism ([Supplementary Fig. S3](#) and [Table 2](#)). Interestingly, in leaves, categories of proteins related to several biological pathways were up-regulated, including stress and defense responses, photosynthesis, translation, gene expression, and cellular component biogenesis, while categories of proteins involved in the functional generation of precursor metabolites and energy, localization, and transport were repressed. In addition, categories of proteins related to specific molecular functions, such as carbohydrate binding, structural constituent of ribosome, and isomerase activity, were up-regulated in response to spaceflight in leaves. However, categories associated with cell structure exhibited abundance in leaves and scarcity in roots. In roots, protein categories associated with several biological processes, such as cofactor metabolism, oxidative stress responses, and cellular lipid metabolism, showed increased abundance. The abundance of protein categories associated with basic molecular functions, such as ATP binding, adenyl ribonucleotide binding, adenyl nucleotide binding, purine nucleoside binding, and nucleoside binding, were also enhanced in roots.

**TABLE 2.**

FUNCTIONAL CATEGORY COMPARISONS AMONG THE DIFFERENTIALLY REGULATED PROTEINS IN ROOTS AND SHOOTS USING PARAMETRIC ANALYSIS OF GENE EXPRESSION

GO Term	Gnt.	Description	CM Information		Leaves			Roots		
			Num.	Leaves	z score	Mean	P value	z score	Mean	P value
GO:0009517	P	response to bacterium	10	red	5.3	2	1.4E-07	-0.89	1	0.93
GO:0051707	P	response to other organism	23	red	3.8	1.6	0.00013	-0.84	0.92	0.4
GO:0009607	P	response to biotic stimulus	24	red	3.8	1.6	0.00017	-0.84	0.93	0.4
GO:0051704	P	multi-organism process	26	red	3.5	1.5	0.00047	-0.92	0.92	0.58
GO:0006352	P	defense response	26	red	3.2	1.5	0.0016	-0.5	0.98	0.62
GO:0015979	P	photosynthesis	11	yellow	2.7	1.6	0.0076	-1.6	0.74	0.15
GO:0006412	P	translation	76	yellow	2.5	1.3	0.013	-1.8	0.9	0.064
GO:0042254	P	ribosome biogenesis	19	yellow	2.5	1.5	0.014	0.11	1.1	0.91
GO:0022813	P	ribonucleoprotein complex biogenesis	19	yellow	2.5	1.5	0.014	0.11	1.1	0.91
GO:0046085	P	cellular component biogenesis	22	yellow	2.4	1.4	0.017	0.39	1.1	0.7
GO:0009059	P	macromolecule biosynthetic process	81	cyan	2.2	3.3	0.025	-2.1	0.88	0.039
GO:0034645	P	cellular macromolecule biosynthetic process	80	cyan	2.2	1.5	0.026	-1.9	0.9	0.055
GO:0010467	P	gene expression	89	cyan	2.1	1.3	1.90E-02	-2.1	0.89	0.038
GO:0009416	P	response to light stimulus	18	cyan	-2	0.96	0.047	-2.3	0.65	0.019
GO:009314	P	response to radiation	18	cyan	-2	0.96	0.047	-2.3	0.65	0.019
GO:0006091	P	generation of precursors / metabolites and energy	17	gray	-2	0.95	0.046	-0.69	1	0.94
GO:0051234	P	establishment of localization	24	gray	-2.4	0.94	0.015	1.1	1.2	0.28
GO:0051179	P	localization	24	gray	-2.4	0.94	1.50E-02	1.1	1.2	0.26
GO:0006810	P	transport	24	gray	-2.4	0.94	1.50E-02	1.1	1.2	0.26
GO:0010246	F	carbohydrate binding	13	yellow	3.2	1.7	1.60E-03	1.1	1.3	0.27
GO:0059735	F	structural constituent of ribosome	68	yellow	2.7	3.3	7.40E-03	-1.8	0.89	0.065
GO:0005198	F	structural molecule activity	75	yellow	2.2	1.5	0.028	-2.2	0.87	0.028
GO:0016853	F	isomerase activity	22	yellow	2.1	1.4	0.035	0.76	1.2	0.44
GO:0005618	C	cell wall	53	red	4.4	1.5	1.1E-05	-0.89	0.96	0.57
GO:0010312	C	external encapsulating structure	54	red	4.3	1.5	1.7E-05	-0.73	0.98	0.46
GO:0043157	C	photosynthetic membrane	20	red	3.6	3.6	0.0003	-1.5	0.8	0.13
GO:0022925	C	cytosolic large ribosomal subunit	29	red	3.4	1.5	0.00072	-1.9	0.8	0.058
GO:0044445	C	cytosolic part	60	cyan	3.2	1.4	0.0012	-2.8	0.79	0.0048
GO:0048046	C	apoplast	18	yellow	3.2	1.6	0.0013	-1.3	0.83	0.2
GO:0009579	C	thylakoid	31	cyan	3.1	1.5	0.0019	-2.1	0.79	0.04
GO:0005576	C	extracellular region	22	cyan	3	1.5	0.0024	-0.63	0.95	0.53
GO:0035279	C	ribosomal subunit	63	cyan	3	1.4	0.0025	-2.2	0.85	0.028
GO:0015934	C	large ribosomal subunit	32	yellow	3	1.4	0.0025	-1	0.92	0.31
GO:0022426	C	cytosolic ribosome	64	cyan	3	1.4	0.0029	-2.9	0.79	0.036
GO:0009941	C	chloroplast envelope	13	yellow	2.8	1.6	0.0049	-0.71	0.9	0.48
GO:0009505	C	plant-type cell wall	30	yellow	2.7	1.4	0.0063	-1.1	0.91	0.29
GO:0005840	C	ribosome	70	cyan	2.6	1.9	0.01	-2	0.88	0.045
GO:0055935	C	plastid thylakoid membrane	15	yellow	2.5	1.5	0.012	-0.46	0.96	0.64
GO:0042651	C	thylakoid membrane	15	yellow	2.5	1.5	0.012	-0.46	0.96	0.64
GO:0009535	C	chloroplast thylakoid membrane	15	yellow	2.5	1.5	0.012	-0.46	0.96	0.64
GO:0030529	C	ribonucleoprotein complex	74	yellow	2.5	1.5	0.013	-1.5	0.92	0.14
GO:0043232	C	intracellular non-membrane-bound organelle	86	cyan	2.5	1.3	0.013	-2.3	0.87	0.019
GO:0043228	C	non-membrane-bound organelle	86	cyan	2.5	1.3	0.013	-2.3	0.87	0.019
GO:0044436	C	thylakoid part	19	gray	2.3	1.4	0.021	-0.32	1	0.75
GO:0031984	C	organelle subcompartment	19	gray	2.3	1.4	0.021	-0.19	1	0.9
GO:0031976	C	plastid thylakoid	19	gray	2.3	1.4	0.021	-0.13	1	0.9
GO:0009534	C	chloroplast thylakoid	19	gray	2.3	1.4	0.021	-0.13	1	0.9
GO:0016620	C	membrane	126	cyan	2.1	1.3	0.032	-2.2	0.91	0.027
GO:0005829	C	cytosol	87	gray	2.1	1.3	0.037	-1.9	0.9	0.053
GO:0044446	C	intracellular organelle part	156	cyan	2	1.3	0.044	-2.1	0.93	0.035
GO:0044422	C	organelle part	156	cyan	2	1.3	0.044	-2.1	0.93	0.035
GO:0005730	C	nucleolus	31	yellow	2	1.4	0.046	-2.8	0.69	0.051
GO:0051186	P	cofactor metabolic process	12	gray	-0.21	1.2	0.83	2.3	1.5	0.024
GO:0006797	P	response to oxidative stress	23	gray	-0.013	1.2	0.99	2.2	1.4	0.025
GO:0044255	P	cellular lipid metabolic process	13	gray	-0.59	2.1	0.6	2.2	1.5	0.029
GO:0009451	P	response to salt stress	15	gray	-0.3	1.1	0.76	-2	0.69	0.05
GO:0050866	P	nucleobase, nucleoside and nucleotide metabolism	21	gray	-0.33	3.2	0.74	-2	0.74	0.046
GO:0009628	P	response to abiotic stimulus	68	cyan	-0.81	1.1	0.42	-3	0.78	0.023
GO:0005524	F	ATP Binding	18	gray	-0.52	1.1	0.6	2.2	1.4	0.028
GO:0032559	F	adenyl ribonucleotide binding	19	gray	-0.35	3.1	0.72	2.1	1.4	0.034
GO:0030554	F	adenyl nucleotide binding	23	gray	-0.23	1.2	0.82	2.1	1.4	0.037
GO:0001883	F	purine nucleoside binding	23	gray	-0.23	1.2	0.82	2.1	1.4	0.037
GO:0001882	F	nucleoside binding	23	gray	-0.23	3.2	0.82	2.1	1.4	0.037
GO:0016491	F	oxidoreductase activity	72	gray	-1.7	1.1	0.098	-2	0.88	0.043
GO:0016785	F	transferase activity, transferring alley or aryl ether	12	gray	1.1	1.4	0.26	-2.1	0.6	0.037
GO:0022927	C	cytosolic small ribosomal subunit	31	yellow	1.2	1.5	0.22	-2.1	0.78	0.058
GO:0015935	C	small ribosomal subunit	31	yellow	1.2	1.5	0.22	-2.1	0.78	0.058
GO:0011981	C	nuclear lumen	33	cyan	1.0	1.3	0.072	-2.5	0.73	0.011
GO:0044428	C	nuclear part	34	cyan	1.7	1.3	0.088	-2.6	0.73	0.01
GO:0070013	C	intracellular organelle lumen	46	cyan	1.8	1.3	0.067	-2.7	0.77	0.008
GO:0045233	C	organelle lumen	46	cyan	1.8	1.3	0.067	-2.7	0.77	0.008
GO:0011974	C	membrane-enclosed lumen	46	cyan	1.8	1.3	0.067	-2.7	0.77	0.008

[Open in a new tab](#)

Yellow-to-red and cyan-to-blue color scales in color mode (CM) indicate that the representation of the proteins encompassed in that term is up- or down-regulated as a group in spaceflight samples relative to ground samples, respectively. Gray means no statistically significant difference among the samples. Number

(Num.) represents the number of genes included in each GO term. For ontology (Ont.), P, F, and C stand for biological process, molecular function, and cellular component, respectively.

Table 2 is available in color online at [www.liebertonline.com/ast](http://www.liebertonline.com/ast).

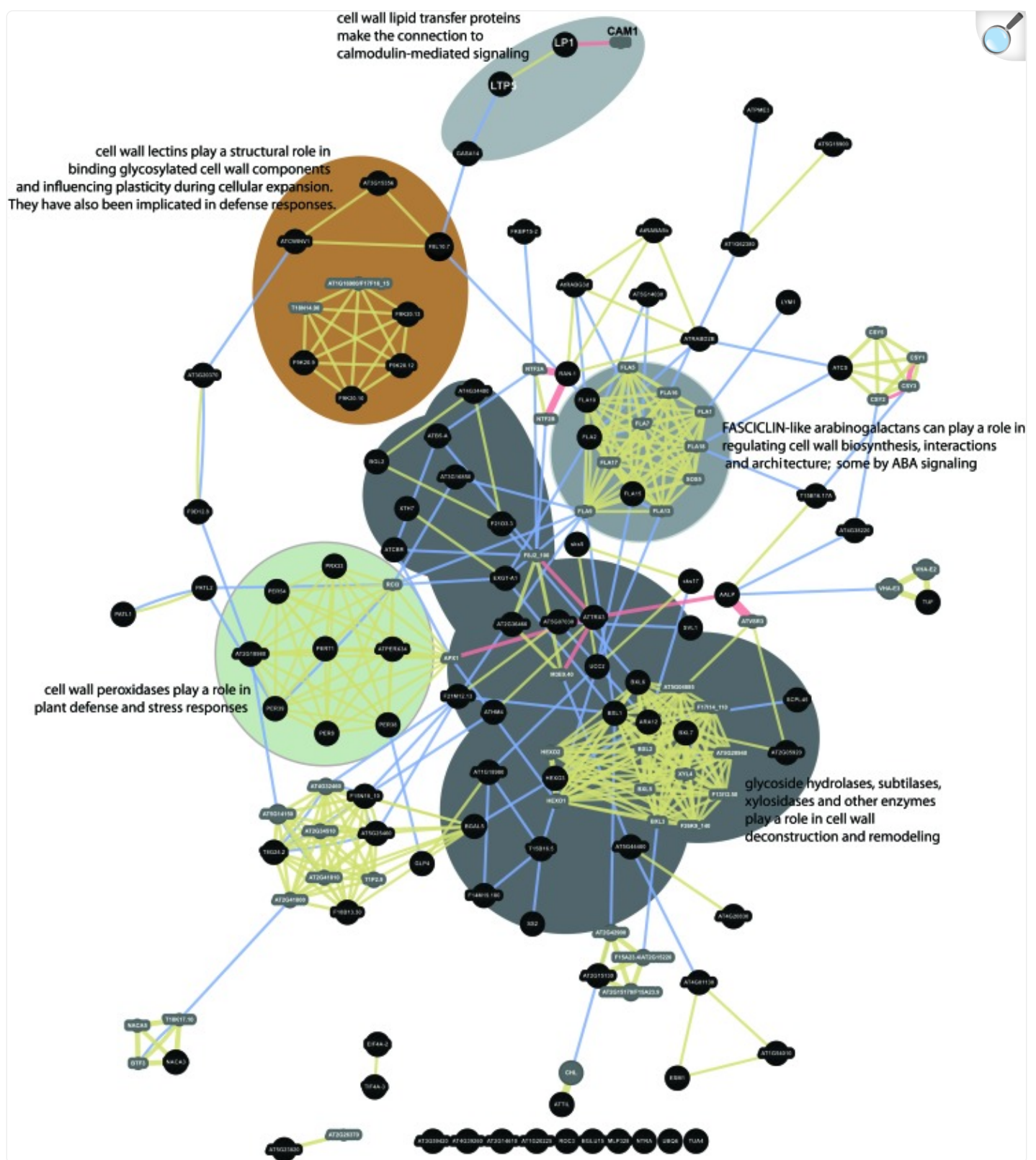
### 3.4. Comparison of proteomic and gene expression data

The proteomics data presented here were derived from *Arabidopsis* grown in Run 1B of the TAGES series of plant growth experiments. Gene expression from microarray data are available from Run 3A of the TAGES experiments (Paul *et al.*, [2013](#)), which involved similar-aged plants grown under very similar conditions on the ISS. The 546 differentially expressed proteins of the present study were compared to the 480 genes exhibiting differential transcript levels in the previous study. The genes encoding most of the proteins quantified in this study did not show a differential mRNA expression, and many of the proteins for genes differentially regulated at the mRNA level were not identified in this proteomics survey. A total of 34 genes exhibited differential expression at both transcript and protein levels. Their transcript and protein fold-change values are compared in [Fig. 5](#). Among the genes and proteins that do show differential expression, there is a positive correlation between direction and degree of differential expression ( $r=0.4901177$ ,  $p$  value=0.0003028;  $r_s=0.5087163$ ,  $p$  value=0.0001618). To examine the degree of concordance between transcript and protein expression levels, correlation tests for which Pearson's  $r$  and Spearman's  $\rho$  ( $r_s$ ) were used were conducted for a direct comparison of proteins and their corresponding transcript expression levels of 34 genes by using log<sub>2</sub>-fold change between ground and flight tissues. As shown in [Fig. 5](#), there is a positive correlation in direction and degree of differential expression between transcript and protein expression ( $r=0.4901177$ ,  $p$  value=0.0003028;  $r_s=0.5087163$ ,  $p$  value=0.0001618).

### 3.5. Cell wall metabolism interaction network

An interaction network was constructed to investigate potential functional relationships among the spaceflight differential proteins that are potentially involved in cell wall interactions and metabolisms. [Figure 6](#) shows the results of the interaction analysis with several key collections of proteins highlighted. Physical interactions, shared protein domains, and co-localizations draw nearly all the cell wall–identified proteins of this study into a codified network that links cell wall carbohydrate enzymology with cell-cell interactions and signaling.

**FIG. 6.**



[Open in a new tab](#)

Interaction network of cell wall-related proteins differentially abundant in spaceflight. Ninety-five proteins identified by SUBA3 as having cell wall-related functions were analyzed by GeneMANIA to provide an interaction network to explore the relationships among the cell wall-related proteins. Black circles indicate the positions of the input proteins from this study. Smaller gray circles indicate proteins brought into the network by the software to provide additional connection resolution. Physical interactions are indicated by red connector lines. Shared physical location is indicated by blue connector lines. Shared protein domains are indicated by beige connector lines. The grouping of cell wall peroxidases is highlighted with a green background. Cell wall lectins are highlighted with a brown background. Lipid transfer proteins and signal connections are highlighted with a light gray background. Fasciclins are highlighted with a medium gray background. A dark gray background highlights enzymes with carbohydrate modifying activities. (Color graphics available online at [www.liebertonline.com/ast](http://www.liebertonline.com/ast) )

## 4. Discussion

---

The technical goal of this study was to test the feasibility of using RNAlater-preserved plant tissue, harvested and frozen on orbit, for broad-scale proteomics analysis of *Arabidopsis* spaceflight responses. RNAlater preservation of *Arabidopsis* within KFTs on orbit is commonly practiced, and a facile process pathway exists for harvesting to RNAlater and frozen sample return from the ISS. RNAlater-preserved plant materials from the ISS have been extensively used for gene expression analyses; however, to date, the use of RNAlater-preserved ISS material for proteomics has been limited to yeast (van Eijnsden *et al.*, 2013). The ability to conduct proteomics analyses on the same samples or on parallel samples returning from this established process pathway would advance the analysis potential for understanding *Arabidopsis* responses to spaceflight.

This study demonstrated that sufficient protein amounts can be isolated from ISS samples preserved in RNAlater to allow broad-scale proteomics studies. Basically, enough protein was recovered from roots and leaves of 12-day-old plants from half a 10 cm<sup>2</sup> Petri plate to conduct proteomic analyses rich enough to return the identities of 1570 proteins and to conduct quantitation on 1432 proteins with iTRAQ methods and relying on at least three unique peptides per protein. Moreover, the methods are sufficiently robust that true biological replicates are consistent and can support statistical methods for evaluation of quantitative differences among sample treatments. These RNAlater iTRAQ methods join frozen native sample recovery and non-isotopic methods (Mazars *et al.*, 2014) as methods that have had successful initial application to space proteomics analyses of plants. It is very likely that the rapid advances in MS currently occurring will raise the number of proteins that can be quantitated in similar future studies that use this or any other sample recovery strategy. And as orbital preservation methods mature and are more broadly applied, informative comparative analyses among various species, growth conditions, and experiment protocols on orbit will become increasingly effective.

The proteomic data from this study of three combined *Arabidopsis* lines support the general notion that plants engage specific metabolic responses to accomplish physiological adaptation to spaceflight, but that response is different among organs (Paul *et al.*, 2013). The primary data supporting this conclusion are shown in Figs. 2 and 4. Of 885 proteins commonly quantified in roots and leaves, only 47 were similarly regulated in the spaceflight leaf and root samples. In contrast, 290 and 288 proteins in roots and leaves were uniquely differentially regulated by spaceflight in either one organ or the other. Moreover, pathway and process analysis of these differentially accumulated proteins indicates that roots and leaves are altering different pathways in response to spaceflight. There appears, broadly speaking, to be no single response at the proteomic level that is employed by all tissues of the plant in order to adapt to spaceflight. There are, however, a few common threads among the data sets.

These data complement results of Mazars *et al.* (2014), who used a non-isotopic proteomics approach to examine spaceflight microgravity effects on membrane proteins of whole *Arabidopsis* seedlings. Their study used seedlings that were grown within chambers in the European Modular Cultivation System (EMCS) for 12 days on the ISS, with the entire chambers frozen on orbit to allow recovery of frozen seedlings after return to Earth. Microsomal fractions were prepared from the whole seedlings and subjected to a label-free MS analysis. Thus, their analysis used different tissues, different preservation on orbit, different sample preparation that focused on microsomes, and different MS methods. Mazars and colleagues found that 69 microsomal proteins were specifically more abundant in microgravity (compared to ground and 1g controls), while 80 microsomal proteins were less abundant in microgravity. By using strictly TAIR AGI accession number as the link between their data and the data presented here, there are 23 proteins identified in common between the two studies. More generally, Mazars *et al.* (2014) concluded that proteins involved in signaling, trafficking, auxin metabolism, stress, and cell wall metabolism are influenced by microgravity, a conclusion that is supported and extended by the study presented here, with auxin signaling and cell wall remodeling being similarly identified here as altered by spaceflight.

Many of the proteins identified here as differentially abundant in spaceflight are associated with auxin metabolism, and a large number are associated with cell wall modification that makes sense in light of the morphologies demonstrated by spaceflight roots (Millar *et al.*, 2011; Paul *et al.*, 2013; Nakashima *et al.*, 2014). Of the differentially represented proteins presented in Table 1, 95 are associated with cell walls or cell wall metabolism either by Gene Ontology annotation or by reference when using SUBA3 searches (Tanz *et al.*, 2013). The interaction network in Fig. 6 shows that most of these cell wall-associated proteins can be considered within a framework of functionally interactive proteins engaged in cell wall activities. There are many enzymes, such as xyloglucan endotransglucosylases, involved in cell wall carbohydrate modification, deconstruction, and remodeling present in the heart of the network (dark gray highlight in Fig. 6) (e.g., Gilbert 2010). The well-represented FASCICLIN-like arabinogalactans (medium gray highlight in Fig. 6) (e.g., Seifert *et al.*, 2014) and a SKU5-like protein are involved in cell shape and cell-cell interactions. For instance, SKU5-similar proteins encode an extracellular glycosylphosphatidylinositol-anchored glycoprotein involved in directional root growth in expanding cells. Mutants in this gene phenocopy the growth patterns seen on orbit in that they over-skew to the left (Sedbrook *et al.*, 2002). FASCICLIN-like arabinogalactans have been shown to positively

modulate ABA-regulated root growth patterns in plants exposed to abiotic stress, and it is postulated that they function by interacting with mediators of ABA in a plasma membrane subdomain (Seifert *et al.*, 2014). Fasciclins are typically associated with the outer face of lipid rafts in the plasma membrane via their GPI (glycosylphosphatidylinositol) anchor (Johnson *et al.*, 2003; Demir *et al.*, 2013). Two cell wall-associated lipid transfer proteins are also differentially represented in the differential spaceflight proteome (light gray highlight in Fig. 6). There is strong representation of cell wall peroxidases (green highlight in Fig. 6) (e.g., Bellincampi *et al.*, 2014) and cell wall lectins (brown highlight in Fig. 6) (e.g., Kauss and Glaser 1974; Albenne *et al.*, 2009) in the network, connecting key metabolism, stress response, and cell expansion activities in the network of proteins differentially regulated by spaceflight. There are also a number of proteins that are connected by a domain of unknown function (DUF) deeply involved in cell wall metabolism (lower left in Fig. 6) (e.g., Garza-Caligaris *et al.*, 2012; Vazquez-Lobo *et al.*, 2012).

These proteomics studies offered an initial opportunity to potentially integrate information on spaceflight responses at the protein and mRNA levels in that these samples were derived from very similar grow-outs on the ISS to the transcriptomics studies of Paul *et al.* (2013). A direct comparison of differential protein levels and their corresponding transcript expression levels does show some correlation. However, only a small portion of the differential transcripts are represented in the differential protein levels, and vice versa. This is, however, in agreement with previous studies in yeast (Futcher *et al.*, 1999; Gygi *et al.*, 1999; Washburn *et al.*, 2003), mice (Tian *et al.*, 2004), *Desulfovibrio vulgaris* (Nie *et al.*, 2006), *E. coli* (Ishihama *et al.*, 2005), *Tragopogon* (Koh *et al.*, 2012), and cotton (Hu *et al.*, 2013), showing that transcript abundances only partially predict protein abundances and that a series of regulatory processes involved in translation, localization, modification, and protein degradation play a substantial role in controlling protein expression (Vogel and Marcotte, 2012). Nonetheless, conclusions based on the proteomics and transcriptomics levels closely interrelate when examining protein name or function as opposed to strict TAIR accession number. The exact same gene/protein may not be represented in the corresponding transcriptome, yet the differential proteome from these samples displays a similar engagement of cell wall remodeling tools in response to spaceflight as seen in the transcriptome from similar samples.

Roots and leaves adapt differently to spaceflight at the level of proteomics. While there are some commonalities among the spaceflight proteome changes in roots and leaves, such as cell wall metabolism, the present data indicate that roots and leaves invoke differential proteome responses to spaceflight. This is consistent with transcriptome data that also indicate differential spaceflight responses in leaves and roots (Paul *et al.*, 2013).

It is likely that, as proteomics technologies as well as gene expression and other omics technologies achieve increased density of coverage and finer spatial resolution, it will be revealed that different cell types within organs respond differently to spaceflight. And as increased numbers of biological experiments are enabled on the ISS, it is likely that multiple approaches will combine to yield both cell-specific response pathways as well as more general principles involved in plant spaceflight adaptation. Cell wall modifications in spaceflight, in addition to or governed by auxin signaling, may be one of those general and recurring metabolic adaptations that may be in common among plants and

plant tissues, even if enacted by various proteins and genes that differ among cell types or genotypes.

## Supplementary Material

---

Supplemental data

[Supp\\_Fig1.pdf](#)(100KB, pdf)

Supplemental data

[Supp\\_Fig2.pdf](#)(52.2KB, pdf)

Supplemental data

[Supp\\_Fig3.pdf](#)(288.5KB, pdf)

## Acknowledgments

---

The authors thank the entire line of NASA space biology professionals that made this research possible. This research was supported by NASA grants NNX07AH270 and NNX09AL96G to R.J.F. and A.-L.P. Agata Zupanska, Eric Schultz, and Natasha Sng contributed to the handling of APEX data and samples. The proteomics analyses were conducted within the Proteomics core laboratory of the Interdisciplinary Center for Biotechnology Research at the University of Florida. The proteomics data are available for public access at the PRIDE Archive—proteomics data repository <http://www.ebi.ac.uk/pride/archive>.

## Disclosure Statement

---

No competing financial interests exist.

## Abbreviations

---

ABRS, Advanced Biological Research System; FDR, false discovery rate; GFP, green fluorescent protein; GIS, GFP Imaging System; ISS, International Space Station; iTRAQ, isotope tags for relative and absolute quantification; KFTs, Kennedy Space Center Fixation Tubes; MS, mass spectrometry; PAGE, parametric analysis of gene set enrichment.

## References

---

1. Albenne C., Canut H., Boudart G., Zhang Y., San Clemente H., Pont-Lezica R., and Jamet E. (2009) Plant cell wall proteomics: mass spectrometry data, a trove for research on protein structure/function relationships. *Mol Plant* 2:977–989 [[DOI](#)] [[PubMed](#)] [[Google Scholar](#)]
2. Alvarez S., Hicks L.M., and Pandey S. (2011) ABA-dependent and -independent G-protein signaling in *Arabidopsis* roots revealed through an iTRAQ proteomics approach. *J Proteome Res* 10:3107–3122 [[DOI](#)] [[PubMed](#)] [[Google Scholar](#)]
3. Bantscheff M., Boesche M., Eberhard D., Mattheson T., Sweetman G., and Kuster B. (2008) Robust and sensitive iTRAQ quantification on an LTQ Orbitrap mass spectrometer. *Mol Cell Proteomics* 7:1702–1713 [[DOI](#)] [[PMC free article](#)] [[PubMed](#)] [[Google Scholar](#)]
4. Bellincampi D., Cervone F., and Lionetti V. (2014) Plant cell wall dynamics and wall-related susceptibility in plant-pathogen interactions. *Front Plant Sci* 5, doi: 10.3389/fpls.2014.00228 [[DOI](#)] [[PMC free article](#)] [[PubMed](#)] [[Google Scholar](#)]
5. Bevan M., Bancroft I., Bent E., Love K., Goodman H., Dean C., Bergkamp R., Dirkse W., Van Staveren M., Stiekema W., Drost L., Ridley P., Hudson S.A., Patel K., Murphy G., Piffanelli P., Wedler H., Wedler E., Wambutt R., Weitzenegger T., Pohl T.M., Terryn N., Gielen J., Villarroel R., De Clerck R., Van Montagu M., Lecharny A., Auborg S., Gy I., Kreis M., Lao N., Kavanagh T., Hempel S., Kotter P., Entian K.D., Rieger M., Schaeffer M., Funk B., Mueller-Auer S., Silvey M., James R., Montfort A., Pons A., Puigdomenech P., Douka A., Voukelatou E., Milioni D., Hatzopoulos P., Piravandi E., Obermaier B., Hilbert H., Dusterhoff A., Moores T., Jones J.D., Eneva T., Palme K., Benes V., Rechman S., Ansorge W., Cooke R., Berger C., Delsenay M., Voet M., Volckaert G., Mewes H.W., Klosterman S., Schueler C., and Chalwatzis N. (1998) Analysis of 1.9 Mb of contiguous sequence from chromosome 4 of *Arabidopsis thaliana*. *Nature* 391:485–488 [[DOI](#)] [[PubMed](#)] [[Google Scholar](#)]
6. Conesa A., Gotz S., Garcia-Gomez J.M., Terol J., Talon M., and Robles M. (2005) Blast2GO: a universal tool for annotation, visualization and analysis in functional genomics research. *Bioinformatics* 21:3674–3676 [[DOI](#)] [[PubMed](#)] [[Google Scholar](#)]

7. Correll M.J., Pyle T.P., Millar K.D., Sun Y., Yao J., Edelmann R.E., and Kiss J.Z. (2013) Transcriptome analyses of *Arabidopsis thaliana* seedlings grown in space: implications for gravity-responsive genes. *Planta* 238:519–533 [[DOI](#)] [[PubMed](#)] [[Google Scholar](#)]
8. Demir F., Hornrich C., Blachutzik J.O., Scherzer S., Reinders Y., Kiersznowska S., Schulze W.X., Harms G.S., Hedrich R., Geiger D., and Kreuzer I. (2013) Arabidopsis nanodomain-delimited ABA signaling pathway regulates the anion channel SLAH3. *Proc Natl Acad Sci USA* 110:8296–8301 [[DOI](#)] [[PMC free article](#)] [[PubMed](#)] [[Google Scholar](#)]
9. DeSouza L.V., Romaschin A.D., Colgan T.J., and Siu K.W. (2009) Absolute quantification of potential cancer markers in clinical tissue homogenates using multiple reaction monitoring on a hybrid triple quadrupole/linear ion trap tandem mass spectrometer. *Anal Chem* 81:3462–3470 [[DOI](#)] [[PubMed](#)] [[Google Scholar](#)]
10. Eng J.K., McCormack A.L., and Yates J.R. (1994) An approach to correlate tandem mass spectral data of peptides with amino acid sequences in a protein database. *J Am Soc Mass Spectrom* 5:976–989 [[DOI](#)] [[PubMed](#)] [[Google Scholar](#)]
11. Ferl R.J., Zupanska A., Spinale A., Reed D., Manning-Roach S., Guerra G., Cox D.R., and Paul A.-L. (2011) The performance of KSC Fixation Tubes with RNALater for orbital experiments: a case study in ISS operations for molecular biology. *Adv Space Res* 48:199–206 [[Google Scholar](#)]
12. Fisher R.A. (1948) Questions and answers #14. *Am Stat* 2:30–31 [[Google Scholar](#)]
13. Futcher B., Latter G.I., Monardo P., McLaughlin C.S., and Garrels J.I. (1999) A sampling of the yeast proteome. *Mol Cell Biol* 19:7357–7368 [[DOI](#)] [[PMC free article](#)] [[PubMed](#)] [[Google Scholar](#)]
14. Garza-Caligaris L.E., Avendano-Vazquez A.O., Alvarado-Lopez S., Zuniga-Sanchez E., Orozco-Segovia A., Perez-Ruiz R.V., and Gamboa-Debuen A. (2012) At3g08030 transcript: a molecular marker of seed ageing. *Ann Bot* 110:1253–1260 [[DOI](#)] [[PMC free article](#)] [[PubMed](#)] [[Google Scholar](#)]
15. Gilbert H.J. (2010) The biochemistry and structural biology of plant cell wall deconstruction. *Plant Physiol* 153:444–455 [[DOI](#)] [[PMC free article](#)] [[PubMed](#)] [[Google Scholar](#)]
16. Gygi S.P., Rochon Y., Franz B.R., and Aebersold R. (1999) Correlation between protein and mRNA abundance in yeast. *Mol Cell Biol* 19:1720–1730 [[DOI](#)] [[PMC free article](#)] [[PubMed](#)] [[Google Scholar](#)]
17. Hu G., Koh J., Yoo M.J., Grupp K., Chen S., and Wendel J.F. (2013) Proteomic profiling of developing cotton fibers from wild and domesticated *Gossypium barbadense*. *New Phytol* 200:570–582 [[DOI](#)] [[PubMed](#)] [[Google Scholar](#)]

18. Ishihama Y., Oda Y., Tabata T., Sato T., Nagasu T., Rappaport J., and Mann M. (2005) Exponentially modified protein abundance index (emPAI) for estimation of absolute protein amount in proteomics by the number of sequenced peptides per protein. *Mol Cell Proteomics* 4:1265–1272 [[DOI](#)] [[PubMed](#)] [[Google Scholar](#)]
19. Johnson K.L., Jones B.J., Bacic A., and Schultz C.J. (2003) The fasciclin-like arabinogalactan proteins of *Arabidopsis*. A multigene family of putative cell adhesion molecules. *Plant Physiol* 133:1911–1925 [[DOI](#)] [[PMC free article](#)] [[PubMed](#)] [[Google Scholar](#)]
20. Karp N.A., Huber W., Sadowski P.G., Charles P.D., Hester S.V., and Lilley K.S. (2010) Addressing accuracy and precision issues in iTRAQ quantitation. *Mol Cell Proteomics* 9:1885–1897 [[DOI](#)] [[PMC free article](#)] [[PubMed](#)] [[Google Scholar](#)]
21. Kauss H., and Glaser C. (1974) Carbohydrate-binding proteins from plant cell walls and their possible involvement in extension growth. *FEBS Lett* 45:304–307 [[DOI](#)] [[PubMed](#)] [[Google Scholar](#)]
22. Koh J., Chen S., Zhu N., Yu F., Soltis P.S., and Soltis D.E. (2012) Comparative proteomics of the recently and recurrently formed natural allopolyploid *Tragopogon mirus* (Asteraceae) and its parents. *New Phytol* 196:292–305 [[DOI](#)] [[PubMed](#)] [[Google Scholar](#)]
23. Li Z., Czarnecki O., Chourey K., Yang J., Tuskan G.A., Hurst G.B., Pan C., and Chen J.G. (2014) Strigolactone-regulated proteins revealed by iTRAQ-based quantitative proteomics in *Arabidopsis*. *J Proteome Res* 13:1359–1372 [[DOI](#)] [[PubMed](#)] [[Google Scholar](#)]
24. Link B.M., Wagner E.R., and Cosgrove D.J. (2001) The effect of a microgravity (space) environment on the expression of expansins from the peg and root tissues of *Cucumis sativus*. *Physiol Plant* 113:292–300 [[DOI](#)] [[PubMed](#)] [[Google Scholar](#)]
25. Makarov A., Denisov E., Lange O., and Horning S. (2006) Dynamic range of mass accuracy in LTQ Orbitrap hybrid mass spectrometer. *J Am Soc Mass Spectrom* 17:977–982 [[DOI](#)] [[PubMed](#)] [[Google Scholar](#)]
26. Manak M.S., Paul A.L., Sehnke P.C., and Ferl R.J. (2002) Remote sensing of gene expression in *Plants*: transgenic plants as monitors of exogenous stress perception in extraterrestrial environments. *Life Support Biosph Sci* 8:83–91 [[PubMed](#)] [[Google Scholar](#)]
27. Mazars C., Briere C., Grat S., Pichereaux C., Rossignol M., Pereda-Loth V., Eche B., Boucheron-Dubuisson E., Le Disquet I., Medina F.J., Graziana A., and Carnero-Diaz E. (2014) Microgravity induces changes in microsome-associated proteins of *Arabidopsis* seedlings grown on board the International Space Station. *PloS One* 9:e91814. [[DOI](#)] [[PMC free article](#)] [[PubMed](#)] [[Google Scholar](#)]

28. Millar K.D., Johnson C.M., Edelmann R.E., and Kiss J.Z. (2011) An endogenous growth pattern of roots is revealed in seedlings grown in microgravity. *Astrobiology* 11:787–797 [[DOI](#)] [[PMC free article](#)] [[PubMed](#)] [[Google Scholar](#)]
29. Moseyko N., Zhu T., Chang H.S., Wang X., and Feldman L.J. (2002) Transcription profiling of the early gravitropic response in *Arabidopsis* using high-density oligonucleotide probe microarrays. *Plant Physiol* 130:720–728 [[DOI](#)] [[PMC free article](#)] [[PubMed](#)] [[Google Scholar](#)]
30. Musgrave M.E., Kuang A., and Matthews S.W. (1997) Plant reproduction during spaceflight: importance of the gaseous environment. *Planta* 203:S177–S184 [[DOI](#)] [[PubMed](#)] [[Google Scholar](#)]
31. Nakashima J., Liao F., Sparks J.A., Tang Y., and Blancaflor E.B. (2014) The actin cytoskeleton is a suppressor of the endogenous skewing behaviour of *Arabidopsis* primary roots in microgravity. *Plant Biology* 16:142–150 [[DOI](#)] [[PubMed](#)] [[Google Scholar](#)]
32. NASA. (2011a) Advanced Biological Research System (ABRS). In International Space Station Fact Sheet, National Aeronautics and Space Administration, Washington, DC, Available online at [http://www.nasa.gov/mission\\_pages/station/research/experiments/ABRS.html](http://www.nasa.gov/mission_pages/station/research/experiments/ABRS.html) [[Google Scholar](#)]
33. NASA. (2011b) Transgenic *Arabidopsis* Gene Expression System (TAGES). In International Space Station Fact Sheet, National Aeronautics and Space Administration, Washington, DC: Available online at [http://www.nasa.gov/mission\\_pages/station/research/experiments/TAGES.html#overview](http://www.nasa.gov/mission_pages/station/research/experiments/TAGES.html#overview) [[Google Scholar](#)]
34. Nasir A., Strauch S.M., Becker I., Sperling A., Schuster M., Richter P.R., Weisskopf M., Ntefidou M., Daiker V., An Y.A., Li X.Y., Liu Y.D., and Lebert M. (2014) The influence of microgravity on *Euglena gracilis* as studied on Shenzhou 8. *Plant Biology* 16(Supplement 1):113–119 [[DOI](#)] [[PubMed](#)] [[Google Scholar](#)]
35. Nie L., Wu G., and Zhang W. (2006) Correlation between mRNA and protein abundance in *Desulfovibrio vulgaris*: a multiple regression to identify sources of variations. *Biochem Biophys Res Commun* 339:603–610 [[DOI](#)] [[PubMed](#)] [[Google Scholar](#)]
36. Paul A.-L., Daugherty C.J., Bihn E.A., Chapman D.K., Norwood K.L., and Ferl R.J. (2001) Transgene expression patterns indicate that spaceflight affects stress signal perception and transduction in *arabidopsis*. *Plant Physiol* 126:613–621 [[DOI](#)] [[PMC free article](#)] [[PubMed](#)] [[Google Scholar](#)]
37. Paul A.-L., Schuerger A.C., Popp M.P., Richards J.T., Manak M.S., and Ferl R.J. (2004) Hypobaric biology: *Arabidopsis* gene expression at low atmospheric pressure. *Plant Physiol* 134:215–223 [[DOI](#)] [[PMC free article](#)] [[PubMed](#)] [[Google Scholar](#)]

38. Paul A.-L., Popp M.P., Gurley W.B., Guy C.L., Norwood K.L., and Ferl R.J. (2005) Arabidopsis gene expression patterns are altered during spaceflight. *Adv Space Res* 36:1175–1181 [[Google Scholar](#)]
39. Paul A.-L., Amalfitano C.E., and Ferl R.J. (2012a) Plant growth strategies are remodeled by spaceflight. *BMC Plant Biol* 12, doi: 10.1186/1471-2229-12-232 [[DOI](#)] [[PMC free article](#)] [[PubMed](#)] [[Google Scholar](#)]
40. Paul A.-L., Zupanska A., Ostrow D.T., Zhang Y., Sun Y., Li J.-L., Shanker S., Farmerie W.G., Amalfitano C.E., and Ferl R.J. (2012b) Spaceflight transcriptomes: unique responses to a novel environment. *Astrobiology* 12:40–56 [[DOI](#)] [[PMC free article](#)] [[PubMed](#)] [[Google Scholar](#)]
41. Paul A.-L., Zupanska A.K., Schultz E.R., and Ferl R.J. (2013) Organ-specific remodeling of the Arabidopsis transcriptome in response to spaceflight. *BMC Plant Biol* 13, doi: 10.1186/1471-2229-13-112 [[DOI](#)] [[PMC free article](#)] [[PubMed](#)] [[Google Scholar](#)]
42. Perkins D.N., Pappin D.J.C., Creasy D.M., and Cottrell J.S. (1999) Probability-based protein identification by searching sequence databases using mass spectrometry data. *Electrophoresis* 20:3551–3567 [[DOI](#)] [[PubMed](#)] [[Google Scholar](#)]
43. Salmi M.L. and Roux S.J. (2008) Gene expression changes induced by space flight in single-cells of the fern *Ceratopteris richardii*. *Planta* 229:151–159 [[DOI](#)] [[PubMed](#)] [[Google Scholar](#)]
44. Salmi M.L., Bushart T.J., and Roux S.J. (2011) Autonomous gravity perception and responses of single plant cells. *Gravit Space Res* 25:6–13 [[Google Scholar](#)]
45. Schenck C.A., Nadella V., Clay S.L., Lindner J., Abrams Z., and Wyatt S.E. (2013) A proteomics approach identifies novel proteins involved in gravitropic signal transduction. *Am J Bot* 100:194–202 [[DOI](#)] [[PubMed](#)] [[Google Scholar](#)]
46. Sedbrook J.C., Carroll K.L., Hung K.F., Masson P.H., and Somerville C.R. (2002) The Arabidopsis *SKU5* gene encodes an extracellular glycosyl phosphatidylinositol–anchored glycoprotein involved in directional root growth. *Plant Cell* 14:1635–1648 [[DOI](#)] [[PMC free article](#)] [[PubMed](#)] [[Google Scholar](#)]
47. Seifert G.J., Xue H., and Acet T. (2014) The *Arabidopsis thaliana FASCICLIN-LIKE ARABINOGALACTAN PROTEIN 4* gene acts synergistically with abscisic acid signalling to control root growth. *Ann Bot* 14:1125–1133 [[DOI](#)] [[PMC free article](#)] [[PubMed](#)] [[Google Scholar](#)]
48. Sheen J., Hwang S., Niwa Y., Kobayashi H., and Galbraith D.W. (1995) Green-fluorescent protein as a new vital marker in plant cells. *Plant J* 8:777–784 [[DOI](#)] [[PubMed](#)] [[Google Scholar](#)]
49. Shilov I.V., Seymour S.L., Patel A.A., Loboda A., Tang W.H., Keating S.P., Hunter C.L., Nuwaysir L.M., and Schaeffer D.A. (2007) The Paragon Algorithm, a next generation search engine that uses sequence

temperature values and feature probabilities to identify peptides from tandem mass spectra. Mol Cell Proteomics 6:1638–1655 [DOI] [PubMed] [Google Scholar]

50. Stutte G.W., Monje O., Hatfield R.D., Paul A.L., Ferl R.J., and Simone C.G. (2006) Microgravity effects on leaf morphology, cell structure, carbon metabolism and mRNA expression of dwarf wheat. Planta 224:1038–1049 [DOI] [PubMed] [Google Scholar]
51. Sugimoto M., Oono Y., Gusev O., Matsumoto T., Yazawa T., Levinskikh M.A., Sychev V.N., Bingham G.E., Wheeler R., and Hummerick M. (2014) Genome-wide expression analysis of reactive oxygen species gene network in Mizuna plants grown in long-term spaceflight. BMC Plant Biol 14, doi: 10.1186/1471-2229-14-4 [DOI] [PMC free article] [PubMed] [Google Scholar]
52. Tan C., Wang H., Zhang Y., Qi B., Xu G., and Zheng H. (2011) A proteomic approach to analyzing responses of *Arabidopsis thaliana* root cells to different gravitational conditions using an agravitropic mutant, *pin2* and its wild type. Proteome Sci 9, doi: 10.1186/1477-5956-9-72 [DOI] [PMC free article] [PubMed] [Google Scholar]
53. Tang W.H., Shilov I.V., and Seymour S.L. (2008) Nonlinear fitting method for determining local false discovery rates from decoy database searches. J Proteome Res 7:3661–3667 [DOI] [PubMed] [Google Scholar]
54. Tanz S.K., Castleden I., Hooper C.M., Vacher M., Small I., and Millar H.A. (2013) SUBA3: a database for integrating experimentation and prediction to define the SUBcellular location of proteins in Arabidopsis. Nucleic Acids Res 41:D1185–D1191 [DOI] [PMC free article] [PubMed] [Google Scholar]
55. Tian Q., Stepaniants S.B., Mao M., Weng L., Feetham M.C., Doyle M.J., Yi E.C., Dai H., Thorsson V., Eng J., Goodlett D., Berger J.P., Gunter B., Linseley P.S., Stoughton R.B., Aebersold R., Collins S.J., Hanlon W.A., and Hood L.E. (2004) Integrated genomic and proteomic analyses of gene expression in mammalian cells. Mol Cell Proteomics 3:960–969 [DOI] [PubMed] [Google Scholar]
56. Ulmasov T., Murfett J., Hagen G., and Guilfoyle T.J. (1997) Aux/IAA proteins repress expression of reporter genes containing natural and highly active synthetic auxin response elements. Plant Cell 9:1963–1971 [DOI] [PMC free article] [PubMed] [Google Scholar]
57. van Eijnsden R.G., Stassen C., Daenen L., Van Mulders S.E., Bapat P.M., Siewers V., Goossens K.V., Nielsen J., Delvaux F.R., Van Hummelen P., Devreese B., and Willaert R.G. (2013) A universal fixation method based on quaternary ammonium salts (RNAlater) for omics-technologies: *Saccharomyces cerevisiae* as a case study. Biotechnol Lett 35:891–900 [DOI] [PubMed] [Google Scholar]
58. Vazquez-Lobo A., Roujol D., Zuniga-Sanchez E., Albenne C., Pinero D., Gamboa de Buen A., and Jamet E. (2012) The highly conserved spermatophyte cell wall DUF642 protein family: phylogeny and first

evidence of interaction with cell wall polysaccharides *in vitro*. Mol Phylogenetic Evol 63:510–520 [[DOI](#)] [[PubMed](#)] [[Google Scholar](#)]

59. Vizcaino J.A., Deutsch E.W., Wang R., Csordas A., Reisinger F., Rios D., Dianes J.A., Sun Z., Farrah T., Bandeira N., Binz P.A., Xenarios I., Eisenacher M., Mayer G., Gatto L., Campos A., Chalkley R.J., Kraus H.J., Albar J.P., Martinez-Bartolome S., Apweiler R., Omenn G.S., Martens L., Jones A.R., and Hermjakob H. (2014) ProteomeXchange provides globally coordinated proteomics data submission and dissemination. Nat Biotechnol 32:223–226 [[DOI](#)] [[PMC free article](#)] [[PubMed](#)] [[Google Scholar](#)]
60. Vogel C. and Marcotte E.M. (2012) Insights into the regulation of protein abundance from proteomic and transcriptomic analyses. Nat Rev Genet 13:227–232 [[DOI](#)] [[PMC free article](#)] [[PubMed](#)] [[Google Scholar](#)]
61. Warde-Farley D., Donaldson S.L., Comes O., Zuberi K., Badrawi R., Chao P., Franz M., Grouios C., Kazi F., Lopes C.T., Maitland A., Mostafavi S., Montojo J., Shao Q., Wright G., Bader G.D., and Morris Q. (2010) The GeneMANIA prediction server: biological network integration for gene prioritization and predicting gene function. Nucleic Acids Res 38:W214–W220 [[DOI](#)] [[PMC free article](#)] [[PubMed](#)] [[Google Scholar](#)]
62. Washburn M.P., Koller A., Oshiro G., Ulaszek R.R., Plouffe D., Deciu C., Winzeler E., and Yates J.R., III (2003) Protein pathway and complex clustering of correlated mRNA and protein expression analyses in *Saccharomyces cerevisiae*. Proc Natl Acad Sci USA 100:3107–3112 [[DOI](#)] [[PMC free article](#)] [[PubMed](#)] [[Google Scholar](#)]
63. Wolff S.A., Coelho L.H., Zabrodina M., Brinckmann E., and Kittang A.-I. (2013) Plant mineral nutrition, gas exchange and photosynthesis in space: a review. Adv Space Res 51:465–475 [[Google Scholar](#)]
64. Zhao Z., Stanley B.A., Zhang W., and Assmann S.M. (2010) ABA-regulated G protein signaling in Arabidopsis guard cells: a proteomic perspective. J Proteome Res 9:1637–1647 [[DOI](#)] [[PubMed](#)] [[Google Scholar](#)]

## Associated Data

---

*This section collects any data citations, data availability statements, or supplementary materials included in this article.*

## Supplementary Materials

Supplemental data

[Supp\\_Fig1.pdf](#) (100KB, pdf)

Supplemental data

[Supp\\_Fig2.pdf](#) (52.2KB, pdf)

Supplemental data

[Supp\\_Fig3.pdf](#) (288.5KB, pdf)

---

Articles from Astrobiology are provided here courtesy of **Mary Ann Liebert, Inc.**